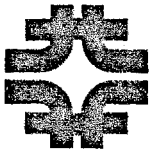

Fermilab

TM-1002
8000.000

A Design of a Slot Type Pick-up for Stochastic Cooling of a Coasting Beam

Part I: Theory and Numerical Values

Hang H. Lai

September, 1980

I. Introduction

Pick-up electrodes for stochastic cooling of particle beam are often suffered either from their frequency limitations or from their low bandwidth characteristics. Furthermore, the induced signal on these electrodes are often very weak and polluted by noise when the particle density is low and the corresponding energy is small. People from Berkeley [1] designed a Traveling Wave Tube type pick-up for the Stochasting cooling experiment here at Fermilab that seemed to be able to overcome the frequency and bandwidth problem. However, it was designed for low energy (200 MeV) coasting beam and thus does not meet the requirement for the high energy experiment intended for the Precooler design. Loop type or wall type pick-ups suggested by Bramham and others [2], because their frequency characteristic, seemed not to satisfy this requirement either. Slot type pick-up was proposed by Faltin [3]. However, its induced signal onto the electrode was found to be very weak and vertical cooling was almost impossible to carry out.

In this report, a design for slot type pick-up and kicker are proposed. A novel analytical approach, as well as a different physical setup and dimensions for the electrodes are presented. Electromagnetic waveguide fields, which are generated by the particle beam in the beam chamber, and their physical interaction mechanism between the beam and the electrodes are derived in details. Coupling and power transfer between the beam and the electrode are also obtained. It will be shown that, because of characteristic of this design, the physical dimension and the interaction mechanism for the pick-up and the kicker are not identically the same.

This report is written in two parts. In the first part, we shall present the theoretical basis for this analysis and the numerical results. Part two of this report deals with the exact dimensions and drawing for the pick-up and kicker. Expressions for the signal induced on pick-up or kicker due to various beam current are also shown.

TABLE OF CONTENTS

II. WAVEGUIDE MODAL FIELDS.

Considering an infinitely long waveguide with cross sectional dimensions axb and situated in the coordinates as shown, slots are cut on its broad side walls. A beam current of finite size in cross section is flowing in the center of the waveguide. The electromagnetc fields inside this waveguide, as well as the waves in the slots, are to be found. Let us, for the moment, assume that the beam current and the slots are not there in the structure. This thus becomes an ideal waveguide with perfectly conducting walls. Bearing in mind that we are looking for waves in a waveguide with a longitudinal current compcnent, hence, there is no Z component magnetc field. Since $\nabla \cdot \vec{H} = 0$, here we assume homogeneous medium and μ = constant, we have

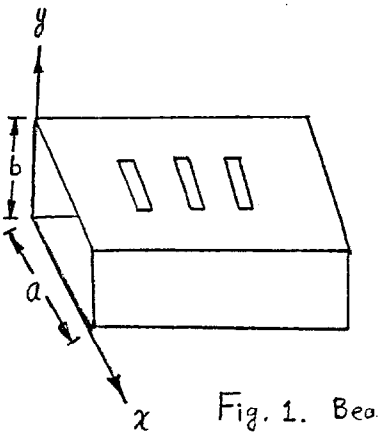

Fig. 1. Beam chamber and its coordinates

$$\frac{\partial}{\partial x} H_x + \frac{\partial}{\partial y} H_y + \frac{\partial}{\partial z} H_z = 0 \qquad (1)$$

These magnetic fields can be derived from a magnetic vector potential $\vec{A}' = A'_z \hat{z}$. Only z component is present for this current element lies in the z direction only [4]. We have $\vec{H} = \nabla \times \vec{A}$

or
$$H_x = \frac{\partial \hat{A}'_z}{\partial y} \quad , \quad H_y = -\frac{\partial \hat{A}'_z}{\partial x} \qquad (2)$$

Here we assume A'_z to be of the form

$$A'_z(x, y, z) = \hat{A}'_z(x, y)\, e^{-j\Gamma' z} \qquad (3)$$

From Maxwell's equation

$$\frac{\partial H_z}{\partial y} - \frac{\partial H_y}{\partial z} = j\omega\epsilon_0 H_x$$

with $\frac{\partial}{\partial z}$ replaced by $-j\Gamma'$, then

$$E_x = \frac{-\Gamma'}{\omega\epsilon_0} \frac{\partial \hat{A}'_z}{\partial x} \qquad (4a)$$

similarly, we have

$$E_y = -\frac{\Gamma'}{\omega\epsilon_0} \frac{\partial \hat{A}'_z}{\partial y} \qquad (4b)$$

We can also apply the Maxwell's equation to obtain E_z, this becomes

$$\frac{\partial H_y}{\partial x} - \frac{\partial H_x}{\partial y} = j\omega\epsilon_o E_z$$

or

$$E_z = \frac{j}{\omega\epsilon_o}\left[\frac{\partial^2}{\partial x^2}\hat{A}'_z + \frac{\partial^2}{\partial y^2}\hat{A}'_z\right] \tag{5}$$

It becomes obvious that if one can find $\hat{A}'_z(x,y)$, then all the waveguide fields will be found by using Eqs. (2), (4) and (5). To this end, we shall use the Maxwell's equation again:

$$\frac{\partial E_z}{\partial y} - \frac{\partial E_y}{\partial z} = -j\omega\mu_o H_x$$

or

$$\frac{\partial}{\partial y}\left[\frac{j}{\omega\epsilon_o}\left(\frac{\partial^2}{\partial x^2}\hat{A}'_z + \frac{\partial^2}{\partial y^2}\hat{A}'_z\right)\right] - \frac{j\Gamma'^2}{\omega\epsilon_o}\frac{\partial\hat{A}'_z}{\partial y} = -j\omega\mu_o\frac{\partial\hat{A}'_z}{\partial y}$$

or

$$\frac{\partial}{\partial y}\left[\frac{j}{\omega\epsilon_o}\left(\frac{\partial^2}{\partial x^2}\hat{A}'_z + \frac{\partial^2}{\partial y^2}\hat{A}'_z\right) - \frac{j\Gamma'^2}{\omega\epsilon_o}\hat{A}'_z + j\omega\mu_o\hat{A}'_z\right] = 0$$

This is certainly true if the quantity inside the bracket is zero, or

$$\left(\frac{\partial^2}{\partial x^2} + \frac{\partial^2}{\partial y^2}\right)\hat{A}'_z = (\Gamma'^2 - \beta_o^2)\hat{A}'_z \tag{6}$$

where
$$\beta_o^2 = \omega^2\mu_o\epsilon_o \tag{7}$$

A solution to Eq. (6) pertinent to Fig. 1 is in the form

$$\hat{A}'_z(x,y) = \hat{A}'_{zmn}(x,y) = \sum_{m=-\infty}^{\infty}\sum_{n=-\infty}^{\infty}\sin\left(\frac{m\pi x}{a}\right)\sin\left(\frac{n\pi y}{b}\right) \tag{8}$$

where
$$\Gamma'^2 = \beta_o^2 - \left(\frac{m\pi}{a}\right)^2 - \left(\frac{n\pi}{b}\right)^2 = \Gamma'^2_{mn} \tag{9}$$

Here, obviously, Γ' is a function of m and n and $\hat{A}'_z(x,y)$ contains both forward and backward travelling waves. The reason for $\hat{A}'_z(x,y)$ in the form of Eq. (8) is because the boundary conditions require that the tangential electric fields are all zero. (eq. (4))

Let us now incorporate a longitudinal current

$$\vec{J} = J_z(x,y)\, e^{-j\Gamma z}\, \hat{z} \tag{10}$$

into the waveguide. Note that this current has only one component, namely, the z component, and it is not necessarily lied in center of the waveguide. Now the Maxwell's equation in the presence of this convection current becomes

$$\frac{\partial H_y}{\partial x} - \frac{\partial H_x}{\partial y} = j\omega \epsilon_o E_z + J_z$$

or

$$E_z = \frac{j}{\omega \epsilon_o}\left(\frac{\partial^2 A_z}{\partial x^2} + \frac{\partial^2 A_z}{\partial y^2}\right) + \frac{j}{\omega \epsilon} J_z \tag{11}$$

Here A_z is the z component of the vector potential of the waveguide in the presence of the beam current. It has the same form as that of the case when the beam current is absent, or

$$A_z(x,y,z) = \hat{A}_z(x,y)\, e^{-j\Gamma z} \tag{12}$$

Using the same technique given in Eq. (5) through (6), we obtain:

$$\frac{\partial^2}{\partial x^2} A_z + \frac{\partial^2}{\partial y^2} A_z = (\Gamma^2 - \beta_o^2) A_z - J_z \tag{13}$$

If we express A_z and J_z in terms of the waveguide characteristic function $\hat{A}'_{zmn}$, i.e.

$$\hat{A}_z = \sum_{m,n=-\infty}^{\infty} C_{mn}\, \hat{A}'_{zmn} = \sum_{m,n} C_{mn} \sin\left(\frac{m\pi x}{a}\right) \sin\left(\frac{n\pi y}{b}\right) \tag{14}$$

and

$$J_z = \sum_{m,n} J_{mn}\, \hat{A}'_{zmn} = \sum_{m,n} J_{mn} \sin\left(\frac{m\pi x}{a}\right) \sin\left(\frac{n\pi y}{b}\right) \tag{15}$$

where

$$J_{mn} = \frac{4}{ab} \int_0^a \int_0^b J_z(x,y) \sin\left(\frac{m\pi x}{a}\right) \sin\left(\frac{n\pi y}{b}\right) dx\, dy \tag{16}$$

From Eq. (6), the fundamental m,nth modal field in the absence of current density is

$$\left(\frac{\partial^2}{\partial x^2}+\frac{\partial^2}{\partial y^2}\right)\hat{A}'_{zmn}(x,y)=\left(\Gamma'^2-\beta_o^2\right)\hat{A}_{zmn}(x,y) \tag{17}$$

while for Eqs. (13) and (14), we have

$$\left(\frac{\partial^2}{\partial x^2}+\frac{\partial^2}{\partial y^2}\right)C_{mn}\hat{A}'_{zmn}(x,y)=C_{mn}\left(\Gamma^2-\beta_o^2\right)\hat{A}'_{zmn}(x,y)-J_{mn}\hat{A}'_{zmn}(x,y) \tag{18}$$

comparing Eqs. (17) and (18), we have

$$C_{mn}=\frac{J_{mn}}{\Gamma^2-\Gamma'^2_{mn}} \tag{19}$$

thus

$$\begin{aligned}A_z&=\sum_{mn}\left[\frac{J_{mn}}{\Gamma^2-\Gamma'^2_{mn}}\hat{A}'_{zmn}(x,y)\right]e^{-j\Gamma z}\\&=\sum_{m,n}\left[\frac{J_{mn}}{\Gamma^2-\Gamma'^2_{mn}}\sin\left(\frac{m\pi x}{a}\right)\sin\left(\frac{n\pi y}{b}\right)\right]e^{-j\Gamma z}\end{aligned} \tag{20}$$

from Eqs. (11) and (13) we see that

$$\begin{aligned}E_z&=\frac{j}{\omega\epsilon_o}\left(\Gamma^2-\beta_o^2\right)A_z\\&=\frac{j\left(\Gamma^2-\beta_o^2\right)}{\omega\epsilon_o}\sum_{m,n}\left[\frac{J_{mn}}{\Gamma^2-\Gamma'^2_{mn}}\sin\left(\frac{m\pi x}{a}\right)\sin\left(\frac{n\pi y}{b}\right)\right]e^{-j\Gamma z}\end{aligned} \tag{21}$$

from Eqs. (4), (5) and (2), we have all the field components created by the beam current

$$E_x=\frac{-\Gamma}{\omega\epsilon_o}\sum_{mn}\frac{J_{mn}\,m\pi}{\left(\Gamma^2-\Gamma'^2_{mn}\right)a}\left[\cos\left(\frac{m\pi x}{a}\right)\sin\left(\frac{n\pi y}{b}\right)\right]e^{-j\Gamma z} \tag{22a}$$

$$E_y=\frac{-\Gamma}{\omega\epsilon_o}\sum_{mn}\frac{J_{mn}\,n\pi}{\left(\Gamma^2-\Gamma'^2_{mn}\right)b}\left[\sin\left(\frac{m\pi x}{a}\right)\cos\left(\frac{n\pi y}{b}\right)\right]e^{-j\Gamma z} \tag{22b}$$

$$H_x = \sum_{mn} \frac{J_{mn}\, n\pi}{(\Gamma^2 - \Gamma_{mn}'^2)\, b} \left[\sin\left(\frac{m\pi x}{a}\right) \cos\left(\frac{n\pi y}{b}\right) \right] e^{-j\Gamma z} \tag{22c}$$

$$H_y = -\sum_{mn} \frac{J_{mn}\, m\pi}{(\Gamma^2 - \Gamma_{mn}'^2)\, a} \left[\cos\left(\frac{m\pi x}{a}\right) \sin\left(\frac{n\pi y}{b}\right) \right] e^{-j\Gamma z} \tag{22d}$$

It is seen from Eqs. (21) and (22) that these fields inside the waveguide are transverse magnetic fields (TM). However, they are by no means regular hollow waveguide modes simply because there is a center beam current in the waveguide. This is in sharp contrast to the result obtained by Faltin [5], who showed that TEM waves were exclusively in the same physical structure. It is easy to visualize that a longitudinal electric field is indeed existed in such a waveguide structure by way of continuity. A hollow waveguide is known to support TM modes, it's E_z component is bound to interact with the longitudinal field existing in the beam current. This interaction is followed in such a fashion that E_z decreases as it walks away from the beam in the transverse direction. Although there may be a discontinuity as it crosses the beam boundary, nonetheless, this field will not diminish to zero until it reaches the waveguide walls, because of the boundary condition requirement. As a matter of fact, this interesting result was derived by Pierce[6], who showed that E_z in this structure is the consequences of the contribution due to the impressed current and the interaction between this current and the fundamental modes of the waveguide. In the following, we shall show this interesting result.

Since

$$\Gamma^2 - \beta_o^2 = (\Gamma^2 - \Gamma_{mn}'^2) + (\Gamma_{mn}'^2 - \beta_o^2)$$

then Eq. (21) becomes

$$E_z = e^{-j\Gamma z} \left\{ \frac{j}{\omega\epsilon_o} \sum_{mn} \frac{(\Gamma_{mn}'^2 - \beta_o^2)\, J_{mn}}{(\Gamma^2 - \Gamma_{mn}'^2)} \sin\left(\frac{m\pi x}{a}\right) \sin\left(\frac{n\pi y}{b}\right) + \frac{j}{\omega\epsilon_o} \sum_{mn} J_{mn} \sin\left(\frac{m\pi x}{a}\right) \sin\frac{n\pi y}{b} \right\}$$

$$= e^{-j\Gamma z} \left\{ \frac{j}{\omega\epsilon_o} \sum_{mn} \frac{(\Gamma_{mn}'^2 - \beta_o^2)\, J_{mn}}{(\Gamma^2 - \Gamma_{mn}'^2)} \sin\left(\frac{m\pi x}{a}\right) \sin\left(\frac{n\pi y}{b}\right) + \frac{j}{\omega\epsilon_o} J_z(x, y) \right\} \tag{23}$$

Eq. (23) clearly shows that the longitudinal electric field for this beam-guide stucture is the result of contributions due to the longitudinal current J_z and the interaction between this current and the fundamental modes of the waveguide. It also shows that there is a sudden drop in E_z as it crosses the boundary of beam current in the transverse plane, for J_z is zero outside the source region. There is a special case where E_z is identically equal to zero (see Eq. (21)), that is when the phase velocity of the wave in the waveguide generated by the beam current is exactly equal to the velocity of light ($\Gamma = \beta_o$). However, this is very unlikely even though as the case in which the velocity of the beam is C_o. This is because the current carriers tended to slow down or speed up, or bunched up, in order to give up some of the energy to the coupling system. In fact this is the operating principle for the longitudinal pick-up designed by the Berkeley people [1].

III. Power Flow in the Beam-Guide.

It is of interest to consider the power carried by the beam in the $+\hat{z}$ direction. This power is

$$P_g = \frac{1}{2}\iint_S \vec{E}\times\vec{H}^*\cdot\hat{z}\,ds$$

$$= \frac{1}{2}\int_0^a\int_0^b \left(E_x H_y^* - E_y H_x^*\right) dx\,dy$$

$$= \frac{1}{2}\int_0^a\int_0^b \frac{\Gamma}{\omega\epsilon_o}\left\{\sum_{m,n=0}^{\infty}\frac{m^2\pi^2 J_{mn}^2}{(\Gamma^2-\Gamma_{mn}'^2)a^2}\cos^2\left(\frac{m\pi x}{a}\right)\sin^2\left(\frac{n\pi y}{b}\right)\right.$$

$$\left. + \sum_{m,n=0}^{\infty}\frac{n^2\pi^2 J_{mn}^2}{(\Gamma^2-\Gamma_{mn}'^2)b^2}\sin^2\left(\frac{m\pi x}{a}\right)\cos^2\left(\frac{n\pi y}{b}\right)\right\} dx\,dy \qquad (24)$$

$$= \frac{\Gamma\pi^2}{8\omega\epsilon_o ab}\sum_{m,n=0}^{\infty}\frac{J_{mn}^2}{(\Gamma^2-\Gamma_{mn}'^2)^2}\left[b^2m^2 + a^2n^2\right]$$

where a * indicates complex conjugate. It is clear that this power depends on the current J_z in the waveguide as well as on the configuration of the waveguide relative to the beam current.

IV. Fields Due to Various Beam Currents.

(1) Infinitesmal cross-sectional beam current.

In this case, an idealized beam current is considered. An infinitesmal small cross-section beam current

$$\vec{J} = I_{z0}\,\delta(x-x_1)\,\delta(y-y_1)\,\hat{z} \tag{25}$$

is located at (x_1,y_1) inside the waveguide. Although this is an idealized case, it is by no means impractical in the experimental sense. A thin wire (compared to wavelength) fed with desired signal at a particular frequency can be used to test this circuit and the theorectical results. This is equivalent to testing the impulse response (or the characteristic) of this device. It is seen from Eq. (15) that

$$J_{mn} = \frac{4}{ab}\int_0^a\int_0^b I_{z0}\,\delta(x-x_1)\,\delta(y-y_1)\sin\left(\frac{m\pi x}{a}\right)\sin\left(\frac{n\pi y}{b}\right)dx\,dy$$

$$= \frac{4\,I_{z0}}{ab}\sin\left(\frac{m\pi x_1}{a}\right)\sin\left(\frac{n\pi y_1}{b}\right) \tag{26}$$

The characteristic vector potential is

$$A_z = \sum_{m,n}\frac{4\,I_{z0}\sin\left(\frac{m\pi x_1}{a}\right)\sin\left(\frac{n\pi y_1}{b}\right)}{ab\left(\Gamma^2-\Gamma'^2_{mn}\right)}\sin\left(\frac{m\pi x}{a}\right)\sin\left(\frac{n\pi y}{b}\right)e^{-\partial\Gamma z} \tag{27}$$

Expressions for individual field components can be found by substituting Eq. (26) into Eq. (21) and (22).

(2) Rectangular cross-section beam current. As shown in the Figure 2†, a uniform rectangular cross-sectional beam is assumed in the waveguide. This beam has a width a_1 and a thickness b_1 and is situated at x_1 and y_1 away from the y and x axes, respectively. In order to simulate a more realistic beam current in the accelerator, we shall follow the technique suggested by Faltin [3]. The Schottky noise current I_{zo} due to a coasting beam of current I_b is

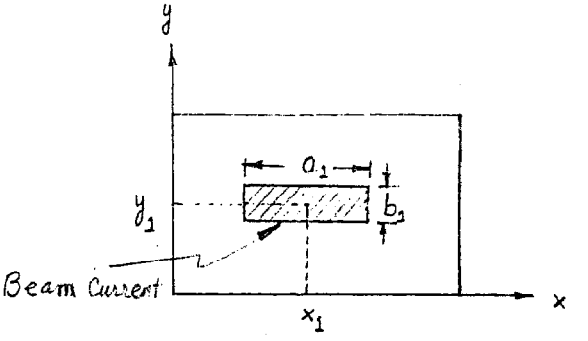

Fig. 2 Location of Beam Current relative to the Chamber.

$$I_{zo} = \sqrt{2e I_b B} \tag{28}$$

where B is the bandwidth of the pickup system. This current in the presence of betatron oscillation becomes

$$I_z = \frac{I_{zo}}{2}\left(1 \pm \cos\nu\omega t\right) e^{j(\omega t - \Gamma z)} \tag{29}$$

Here, we have in effect subdivided the current into two-halves with equal amplitudes but with different time-phase. Referring to Fig. 2 the current density is

$$J_z = \begin{cases} \dfrac{I_{zo}}{a_1 b_1}\left(1+\cos\nu\omega t\right) e^{j(\omega t-\Gamma z)} & \text{for } \begin{cases} x_1 - \frac{a_1}{2} \le x \le x_1 + a_1/2 \\ y_1 \le y \le y_1 + \frac{b_1}{2} \end{cases} \\ \dfrac{I_{zo}}{a_1 b_1}\left(1-\cos\nu\omega t\right) e^{j(\omega t-\Gamma z)} & \text{for } \begin{cases} x_1 - \frac{a_1}{2} \le x \le x_1 + a_1/2 \\ y_1 - \frac{b_1}{2} y \le y \le y_1 \end{cases} \end{cases} \tag{30}$$

---

† We shall adopt the notation convention as follows: (1) Variables without subscripts refer to the beam guide, e.g. a, b; (2) Variables with a subscript "1" refer to the beam current, e.g., a_1, b_1; (3) Variables with subscript "2" refer to values in the coaxial line, e.g. a_2, b_2; (4) Variables with subscript "3" refer to values associated with the slot.

The Fourier counter parts of these currents are (omitting the phase factor):

$$J_{mn} = \frac{4}{ab}\frac{I_{z0}}{a_1 b_1}\int_{x_1-a_1/2}^{x_1+a_1/2} dx \int_{y_1}^{y_1+b_1/2} dy \left(1+\cos\nu\omega t\right)\sin\left(\frac{m\pi x}{a}\right)\sin\left(\frac{n\pi y}{b}\right)$$

$$+ \frac{4}{ab}\frac{I_{z0}}{a_1 b_1}\int_{x_1-a_1/2}^{x_1+a_1/2} dx \int_{y_1-b_1/2}^{y_1} dy \left(1-\cos\nu\omega t\right)\sin\left(\frac{m\pi x}{a}\right)\sin\left(\frac{n\pi y}{b}\right)$$

$$= \frac{4}{ab}\frac{I_{z0}}{a_1 b_1}\left\{\int_{x_1-a_1/2}^{x_1+a_1/2} dx \int_{y_1-b_1/2}^{y_1+b_1/2} dy \sin\left(\frac{m\pi x}{a}\right)\sin\left(\frac{n\pi y}{b}\right)\right.$$

$$\left. + \cos\nu\omega t \int_{x_1-a_1/2}^{x_1+a_1/2} dx \left[\int_{y_1}^{y_1+b_1/2} dy + \int_{y_1}^{y_1-b_1/2} dy\right]\sin\left(\frac{m\pi x}{a}\right)\sin\left(\frac{n\pi y}{b}\right)\right\}$$

$$= \frac{4\,I_{z0}}{mn\pi^2 a_1 b_1}\left\{\left[\cos\frac{m\pi(x_1+a_1/2)}{a}-\cos\frac{m\pi(x_1-a_1/2)}{a}\right]\left[\cos\frac{n\pi(y_1+b_1/2)}{b}-\cos\frac{n\pi(y_1-b_1/2)}{b}\right]\right.$$

$$+\cos\nu\omega t\left[\cos\frac{m\pi(x_1+a_1/2)}{a}-\cos\frac{m\pi(x_1-a_1/2)}{a}\right]\left[\cos\frac{n\pi(y_1+b_1/2)}{b}-\cos\frac{n\pi(y_1-b_1/2)}{b}\right.$$

$$\left.\left.-2\cos\left(\frac{n\pi y_1}{b}\right)\right]\right\}$$

$$= \frac{16\,I_{z0}}{mn\pi^2 a_1 b_1}\sin\frac{m\pi x_1}{a}\sin\frac{m\pi a_1}{2a}\left\{\sin\frac{n\pi y_1}{b}\sin\frac{n\pi b_1}{2b}+\cos\nu\omega t\cos\frac{n\pi y_1}{b}\right.$$

$$\left.\left[1-\cos\frac{n\pi b_1}{2b}\right]\right\} \qquad (31)$$

Again, the electromagnetic field components due to this current can be found by substituting Eq. (31) into Eqs. (21) and (22). It is interesting to observe that from Eq. (31), there are two current components contributing to the EM fields. One is due to the Schottky current e^{jwt} and the other due to the betatron oscillation, the term associated with $\cos\nu\omega t$. They are what is now known as the common mode and the push-pull modal field. It is also interesting to see that these two modal fields are identifiable and separable from the pickup signal because their frequencies are different. It is the push-pull mode

that we are interested in the vertical stochastic cooling experiment. We shall elavorate more about this latter in the second part of this write-up.

(3) An elliptical cross-sectional current. To further simulate the beam current in the accelerator more realistically, it is assumed the beam current is uniformly distributed in an ellipse. As shown in Fig. 3, an ellipse with axes length a_1 and b_1 is centered at (x_1, y_1) inside the waveguide. Following the same technique as given in case 2 (rectangular beam), the current density now becomes

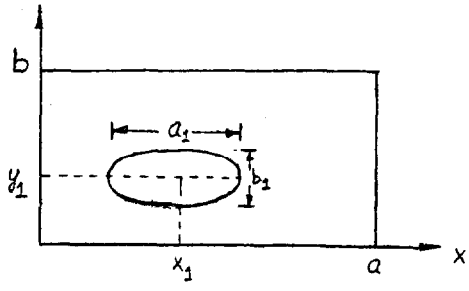

Fig. 3. Elliptical beam in Beam chamber.

Ellipse area $= \pi a_1 b_1$

Eq. $b_1^2 (x-x_1)^2 + a_1^2 (y-y_1) = a_1^2 b_1^2$

$$J_z = \begin{cases} \dfrac{I_{z0}}{\pi a_1 b_1} (1+\cos\nu\omega t)\, e^{j(\omega t - \Gamma z)} & \text{for } \begin{cases} x_1 - \frac{a_1}{2} \le x \le x_1 + \frac{a_1}{2} \\ y_1 \le y \le y_1 + \frac{b_1}{a_1}\sqrt{a_1^2 - (x-x_1)^2} \end{cases} \\ \dfrac{I_{z0}}{\pi a_1 b_1} (1-\cos\nu\omega t)\, e^{j(\omega t - \Gamma z)} & \text{for } \begin{cases} x_1 - \frac{a_1}{2} \le x \le x_1 + \frac{a_1}{2} \\ y_1 - \frac{b_1}{a_1}\sqrt{a_1^2 - (x-x_1)^2} \le y \le y_1 \end{cases} \end{cases} \tag{32}$$

Thus, this Fourier current is

$$J_{mn} = \frac{4}{ab}\frac{I_{z0}}{\pi a_1 b_1}(1+\cos\nu\omega t)\int_{x_1-\frac{a_1}{2}}^{x_1+\frac{a_1}{2}} dx \int_{y_1}^{y_1+\frac{b_1}{a_1}\sqrt{a_1^2-(x-x_1)^2}} dy \sin\left(\frac{m\pi x}{a}\right)\sin\left(\frac{n\pi y}{b}\right)$$

$$+ \frac{4}{ab}\frac{I_{z0}}{\pi a_1 b_1}(1-\cos\nu\omega t)\int_{x_1-\frac{a_1}{2}}^{x_1+\frac{a_1}{2}} dx \int_{y_1-\frac{b_1}{a_1}\sqrt{a_1^2-(x-x_1)^2}}^{y_1} dy \sin\left(\frac{m\pi x}{a}\right)\sin\left(\frac{n\pi y}{b}\right)$$

$$= \frac{4 I_{z0}}{ab\pi a_1 b_1}\left\{\int_{x_1-\frac{a_1}{2}}^{x_1+\frac{a_1}{2}} dx \int_{y_1-\frac{b_1}{a_1}\sqrt{a_1^2-(x-x_1)^2}}^{y_1+\frac{b_1}{a_1}\sqrt{a_1^2-(x-x_1)^2}} dy \sin\left(\frac{m\pi x}{a}\right)\sin\left(\frac{n\pi y}{b}\right)\right.$$

$$\left. + \cos\nu\omega t \int_{x_1-\frac{a_1}{2}}^{x_1+\frac{a_1}{2}} dx \left[\int_{y_1}^{y_1+\frac{b_1}{a_1}\sqrt{a_1^2-(x-x_1)^2}} dy \sin\left(\frac{m\pi x}{a}\right)\sin\left(\frac{n\pi y}{b}\right) + \int_{y_1-\frac{b_1}{a_1}\sqrt{a_1^2-(x-x_1)^2}}^{y_1} dy \sin\left(\frac{m\pi x}{a}\right)\sin\left(\frac{n\pi y}{b}\right)\right]\right\}$$

$$= \frac{4I_{z0}}{n\pi^2 a a_1 b_1}\left\{ \int_{x_1-\frac{a_1}{2}}^{x_1+\frac{a_1}{2}} dx \sin\left(\frac{m\pi x}{a}\right)\left[-\cos\frac{n\pi}{b}\left(y_1+\frac{b_1}{a_1}\sqrt{a_1^2-(x-x_1)^2}\right)\right.\right.$$

$$\left. + \cos\frac{n\pi}{b}\left(y_1-\frac{b_1}{a_1}\sqrt{a_1^2-(x-x_1)^2}\right)\right] + \cos\psi\omega t \int_{x_1-\frac{a_1}{2}}^{x_1+\frac{a_1}{2}} dx \sin\left(\frac{m\pi x}{a}\right)$$

$$\cdot\left[-\cos\frac{n\pi}{b}\left(y_1-\frac{b_1}{a_1}\sqrt{a_1^2-(x-x_1)^2}\right)-\cos\frac{n\pi}{b}\left(y_1-\frac{b_1}{a_1}\sqrt{a_1^2-(x-x_1)^2}\right)\right.$$

$$\left.\left. + 2\cos\left(\frac{n\pi}{b}y_1\right)\right]\right\}$$

$$= \frac{8I_{z0}}{n\pi^2 a a_1 b_1}\left\{ a_1\cos\phi J_1(z)\sin\frac{m\pi x_1}{a}\sin\frac{n\pi y_1}{b} - 2\cos\psi\omega t\sin\frac{m\pi x_1}{a}\cos\frac{n\pi y_1}{b}\right.$$

$$\left.\left[\frac{a_1\sin\phi}{z}\sin(z\sin\phi) + a_1\cos^2\phi J_0(z) + 2\cos\left(\frac{n\pi y_1}{b}\right)\sin\frac{m\pi x_1}{a}\sin\frac{m\pi a_1}{2a}\right]\right\} \quad (33$$

Where

$$\begin{cases} \phi = \tan^{-1}(f/e), \quad e = \dfrac{n\pi b_1}{a_1 b} \\ f = \dfrac{m\pi}{a}, \quad z = a_1\sqrt{e^2+f^2} \\ J_0(z) = \text{Bessel function of the first kind, zero order.} \end{cases} \quad (34)$$

Results in Eq. (33) are derived in details in Appendix A and B.

It is interesting to note that the term associated with betatron motion is retained in this Fourier current element, and that this Fourier current is zero if the center of the ellipse is located at the center of beam chamber i.e. $(x_1, y_1) = (\frac{a}{2}, \frac{b}{2})$ and $m = n = 1$.

V. Fields in the TEM Line.

Expressions for the characteristic impedance and the field configurations in an infinitely extended TEM line have been found by Begovich [7]. However, in order to find the coupling coefficient between the beam chamber and the TEM line, we shall find a rigorous solution to the field expressions for a finite size TEM line by matching the boundary conditions on the conductors [8,9].

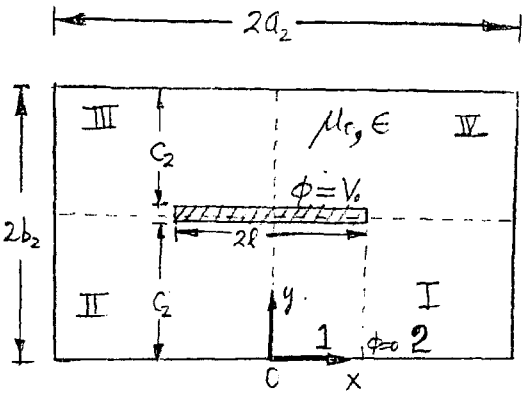

Fig. 4 TEM line and its field boundary condition in Region I

Figure 4 shows a rectangular coaxial line that is coupled to the beam guide. Let us now temporarily assume that there is no slot on the broad side wall and the conductivity is infinite on the out-side wall as well as in the center conductor. In view of the symmetry of the line, we need only to find the field distribution for one quarter of the cross section as in Fig. 4 with potential $\phi(x,y)$ satisfying the following boundary conditions:

$$\phi(x,y) = 0 \quad \text{for} \quad y=0 \text{ and } x=a_2,\ 0\le y\le b_2 \tag{35a}$$

$$\phi(x,y) = V_0 \quad \text{on inner conductor} \tag{35b}$$

$$E_x = -\frac{\partial\phi}{\partial x} = 0 \quad \text{on} \quad x=0,\quad 0\le y\le C_2 \tag{35c}$$

$$E_y = -\frac{\partial\phi}{\partial y} = 0 \quad \text{on} \quad y=b_2,\ \ell\le x\le a_2,\ x=a_2,\ 0\le y\le b_2 \tag{35d}$$

The general solution to the Laplace's equation for these potential functions subjected to boundary conditions are

$$\phi_1(x,y) = \sum_{m=1}^{\infty} A_m \cosh\frac{m\pi x}{C_2}\sin\frac{m\pi y}{C_2} + \frac{V_0 y}{C_2} \quad \text{for} \quad 0\le x\le\ell,\ 0\le y\le C_2 \tag{36}$$

$$\phi_2(x,y) = \sum_{n=\text{odd}}^{\infty} B_n \sinh\left[\frac{n\pi}{2b_2}(a_2-x)\right]\sin\frac{n\pi y}{2b_2} \quad \text{for} \quad \ell\le x\le a_2,\ 0\le y\le b_2 \tag{37}$$

The unknown constants A_m and B_n can be determined by assuring the potential and the electric fields are continuous across the boundary separating regions (1) and (2). Continuity of the potential at $x=\ell$ gives

$$\sum_{m=1}^{\infty} A_m \cosh\frac{m\pi\ell}{c_2} \sin\frac{m\pi y}{c_2} + \frac{V_0 y}{c_2} = \sum_{n=\text{odd}}^{\infty} B_n \sinh\left[\frac{n\pi}{2b_2}(a_2-\ell)\right] \sin\frac{n\pi y}{2b_2} \qquad \text{for} \quad 0 \le y \le c_2 \tag{38}$$

The continuity of E_x is ensured by making $\frac{\partial\phi}{\partial x}$ continuous at $x = \ell$,

$$\sum_{m=1}^{\infty} A_m \frac{m\pi}{c_2} \sinh\frac{m\pi\ell}{c_2} \sin\frac{m\pi y}{c_2} = \sum_{n=\text{odd}}^{\infty} -B_n \frac{n\pi}{2b_2} \cosh\left[\frac{n\pi}{2b_2}(a_2-\ell)\right] \sin\frac{n\pi y}{2b_2} \tag{39}$$

for

$$0 \le y \le c_2$$

To determine A_m, we shall multiply both sides of Eq. (38) by $\text{Sin}(\frac{Py}{c_2})$ and integrate over the interval $(0, c_2)$ and make use of the orthogonality property of trigonmetric functions, we have

$$\frac{c_2}{2} A_p \cosh\frac{p\pi\ell}{c_2} + \int_0^{c_2} \frac{V_0 y}{c_2} \sin\frac{p\pi y}{c_2}\, dy = \sum_{n=\text{odd}}^{\infty} \int_0^{c_2} B_n \sinh\left[\frac{n\pi}{2b_2}(a_2-\ell)\right] \sin\frac{n\pi y}{2b_2} \sin\frac{p\pi y}{c_2}\, dy$$

or

$$\frac{c_2}{2} A_p \cosh\frac{p\pi\ell}{c_2} + \frac{V_0 c_2}{\pi}\left[\frac{(-1)^{p+1}}{p}\right] = \sum_{n=\text{odd}}^{\infty} B_n \sinh\left[\frac{n\pi}{2b_2}(a_2-\ell)\right] \frac{1}{2}\left\{ \frac{\sin\left[\left(\frac{n}{2b_2}-\frac{p}{c_2}\right)\pi c_2\right]}{\left(\frac{n\pi}{2b_2}-\frac{p\pi}{c_2}\right)} - \frac{\sin\left[\left(\frac{n}{2b_2}+\frac{p}{c_2}\right)\pi c_2\right]}{\left(\frac{n\pi}{2b_2}+\frac{p\pi}{c_2}\right)} \right\}$$

$$= \sum_{n=odd}^{\infty} B_n \sinh\left[\frac{n\pi}{2b_2}(a_2-\ell)\right] \frac{(4b_2^2/c_2)\, p \sin\left(\frac{n\pi c_2}{2b_2}\right)(-1)^p}{\pi\left[n^2-\left(\frac{2b_2}{c_2}\right)^2 p^2\right]}$$

or

$$A_p \cosh\left(\frac{p\pi\ell}{c_2}\right)$$

$$= \frac{2V_0}{\pi}\left[\frac{(-1)^p}{p}\right] + \sum_{n=odd}^{\infty} B_n \sinh\left[\frac{n\pi}{2b_2}(a_2-\ell)\right] \frac{(8b_2^2/c_2^2)\, p \sin\left(\frac{n\pi c_2}{2b_2}\right)(-1)^p}{\pi\left[n^2-\left(\frac{2b_2}{c_2}\right)^2 p^2\right]} \qquad (40)$$

Similarly, multiplying both sides of Eq(39) by $\sin\left(\frac{py}{c_2}\right)$ and integrating over the interval $(0,c_2)$, we have

$$\frac{c_2}{2} A_p \frac{p\pi}{c_2} \sinh\frac{p\pi\ell}{c_2}$$

$$= \sum_{n=odd}^{\infty} -B_n \frac{n\pi}{2b_2} \cosh\left[\frac{n\pi}{2b_2}(a_2-\ell)\right] \int_0^{c_2} \sin\frac{n\pi y}{2b_2} \sin\frac{p\pi y}{c_2}\, dy$$

$$= \sum_{n=odd}^{\infty} -B_n \frac{n\pi}{2b_2} \cosh\left[\frac{n\pi}{2b_2}(a_2-\ell)\right] \frac{\frac{p\pi}{c_2}\, 4b_2^2 \sin\left(\frac{n\pi c_2}{2b_2}\right)(-1)^p}{\pi^2\left[n^2-\left(\frac{2b_2}{c_2}\right)^2 p^2\right]} \qquad (41)$$

or

$$A_p \sinh\left(\frac{p\pi\ell}{c_2}\right)$$

$$= \sum_{n=odd}^{\infty} -B_n \cosh\left[\frac{n\pi}{2b_2}(a_2-\ell)\right] \frac{4b_2^2\, n \sin\left(\frac{n\pi c_2}{2b_2}\right)(-1)^p}{c_2\pi\left[n^2-\left(\frac{2b_2}{c_2}\right)^2 p^2\right]} \qquad (42)$$

Taking the ratio of Eq. (40) to (42), we have

$$\sum_{n=odd}^{\infty} -B_n \cosh\left[\frac{n\pi}{2b_2}(a_2-\ell)\right] \frac{4b_2 n \sin\left(\frac{n\pi c_2}{2b_2}\right)(-1)^p \coth\left(\frac{p\pi\ell}{c_2}\right)}{c_2\pi\left[n^2-\left(\frac{2b_2}{c_2}\right)^2 p^2\right]}$$

$$= \frac{2V_0}{\pi}\left[\frac{(-1)^p}{p}\right] + \sum_{n=odd}^{\infty} B_n \sinh\left[\frac{n\pi}{2b_2}(a_1-\ell)\right] \frac{(8b_2^2/c_2^2)\, p \sin\left(\frac{n\pi c_2}{2b_2}\right)(-1)^p}{\pi\left[n^2 - \left(\frac{2b_2}{c_2}\right)^2 p^2\right]}$$

or

$$\sum_{n=odd}^{\infty} B_n \left\{ \frac{2\left(\frac{b_2}{c_2}\right)\sin\left(\frac{n\pi c_2}{2b_2}\right)}{\left[n^2 - \left(\frac{2b_2}{c_2}\right)^2 p^2\right]} \left[n \coth\left(\frac{p\pi\ell}{c_2}\right)\cosh\left[\frac{n\pi}{2b_2}(a_2-\ell)\right] + \frac{2b_2\, p}{c_2}\sinh\left[\frac{n\pi}{2b_2}(a_2-\ell)\right]\right]\right\} + \frac{V_0}{p} = 0 \qquad (43)$$

Setting the value of p=1, then Eq. (43) becomes

$$\sum_{n=odd}^{\infty} B_n \frac{-\left(\frac{2b_2}{c_2}\right)\sin\left(\frac{n\pi c_2}{2b_2}\right)\left\{ n\coth\left(\frac{\pi\ell}{c_2}\right)\cosh\frac{n\pi}{2b_2}(a_2-\ell) + \frac{2b_2}{c_2}\sinh\left[\frac{n\pi}{2b_2}(a_2-\ell)\right]\right\}}{V_0\left[n^2 - \left(\frac{2b_2}{c_2}\right)^2\right]} = 1 \qquad (44)$$

This is equivalent to the form

$$\sum_{n=odd}^{\infty} B_n f_n = 1 \qquad (45)$$

where f_n is a function of n as defined in Eq. (44). Hence, B_n's and f_n's are orthonormal functions. A simple solution to Eq. (45) is

$$B_n = \lim_{N\to\infty} \frac{1}{f_n N} \qquad (46)$$

thus,

$$B_n = \lim_{N\to\infty} \frac{-V_0\left[n^2 - \left(\frac{2b_2}{c_2}\right)^2\right]}{N\left(\frac{2b_2}{c_2}\right)\sin\left(\frac{n\pi c_2}{2b_2}\right)\left\{ n\coth\left(\frac{\pi\ell}{c_2}\right)\cosh\left[\frac{n\pi}{2b_2}(a_2-\ell)\right] + \frac{2b_2}{c_2}\sinh\left[\frac{n\pi}{2b_2}(a_2-\ell)\right]\right\}} \qquad (47a)$$

Substituting this into Eq.(40), we have

$$A_m = \operatorname{sech}\left(\frac{m\pi\ell}{c_2}\right)\frac{V_0}{\pi}(-1)^m\left\{\frac{2}{m} - \sum_{n=odd}^{2N-1} \frac{4\left[n^2 - \left(\frac{2b_2}{c_2}\right)^2\right]\left(\frac{b_2}{c_2}\right)m}{\left[n^2 - \left(\frac{2b_2}{c_2}\right)^2 m^2\right]N\left[n\coth\left(\frac{\pi\ell}{c_2}\right)\coth\left[\frac{n\pi}{2b_2}(a_2-\ell)\right] + \left(\frac{2b_2}{c_2}\right)\right]}\right\} \qquad (47$$

With B_n given in Eq. (47), and A_p in (40). One can determine the field in Region I of the TEM line uniquely. Fields in the other three regions can also be found by symmetrical considerations, they are:

$$\begin{cases} \Phi_1(x,y) = \sum_{m=1}^{\infty} A_m \cosh\frac{m\pi x}{c_2}\sin\frac{m\pi y}{c_2} + \frac{V_0 y}{c_2} & \text{for } \begin{cases} -\ell \le x \le 0 \\ 0 \le y \le c_2 \end{cases} \\ \Phi_2(x,y) = \sum_{n=odd}^{2N-1} B_n \sinh\left[\frac{n\pi}{2b_2}(a_2+x)\right]\sin\frac{n\pi y}{2b_2} & \text{for } \begin{cases} -a_2 \le x \le -\ell \\ 0 \le y \le b_2 \end{cases} \end{cases} \qquad (48)$$

$$\begin{cases} \Phi_1(x,y) = \sum_{m=1}^{\infty} A_m \cosh\frac{m\pi x}{c_2} \sin\frac{m\pi(2b_2-y)}{c_2} + \frac{V_0(2b_2-y)}{c_2} & \text{for } \begin{cases} \ell \geq x \geq 0 \\ (2b_2-c_2) \leq y \leq 2b_2 \end{cases} \\ \Phi_2(x,y) = \sum_{n=\text{odd}}^{2N-1} B_n \sinh\left[\frac{n\pi}{2b_2}(a_2-x)\right] \sin\left[\frac{n\pi(2b_2-y)}{2b_2}\right] & \text{for } \begin{cases} \ell \leq x \leq a_2 \\ (2b_2-c_2) \leq y \leq 2b_2 \end{cases} \end{cases} \tag{49}$$

$$\begin{cases} \Phi_1(x,y) = \sum_{m=1}^{\infty} A_m \cosh\left(\frac{m\pi x}{c_2}\right) \sin\frac{m\pi(2b_2-y)}{c_2} + \frac{V_0(2b_2-y)}{c_2} & \text{for } \begin{cases} -\ell \leq x \leq 0 \\ (2b_2-c_2) \leq y \leq 2b_2 \end{cases} \\ \Phi_2(x,y) = \sum_{n=\text{odd}}^{2N-1} B_n \sinh\left[\frac{n\pi}{2b_2}(a_2+x)\right] \sin\left[\frac{n\pi(2b_2-y)}{2b_2}\right] & \text{for } \begin{cases} -a_2 \leq x \leq -\ell \\ (2b_2-c_2) \leq y \leq 2b_2 \end{cases} \end{cases} \tag{50}$$

where A_m and B_n are defined in Eqs. (47) and (40).

It will be shown later that explicit expressions of the electric and magnetic fields in the TEM line are beneficial for calculations in the following. They are given below:

$$E_x = -\frac{\partial}{\partial x}\Phi(x,y)$$

$$= \begin{cases} -\sum_{m=1}^{\infty} A_m \frac{m\pi}{c_2} \sinh\frac{m\pi x}{c_2} \sin\frac{m\pi y}{c_2} & \text{for } \begin{cases} 0 \leq x \leq \ell \\ 0 \leq y \leq c_2 \end{cases} \\ \sum_{n=\text{odd}}^{2N-1} B_n \frac{n\pi}{2b_2} \cosh\left[\frac{n\pi}{2b_2}(a_2-x)\right] \sin\frac{n\pi y}{2b_2} & \text{for } \begin{cases} \ell \leq x \leq a_2 \\ 0 \leq y \leq b_2 \end{cases} \end{cases} \tag{51a}$$

$$E_y = -\frac{\partial}{\partial y}\Phi(x,y)$$

$$= \begin{cases} -\sum_{m=1}^{\infty} A_m \frac{m\pi}{c_2} \cosh\frac{m\pi x}{c_2} \cos\frac{m\pi y}{c_2} - \frac{V_0}{c_2} & \text{for } \begin{cases} 0 \leq x \leq \ell \\ 0 \leq y \leq c_2 \end{cases} \\ -\sum_{n=\text{odd}}^{2N-1} B_n \frac{n\pi}{2b_2} \sinh\left[\frac{n\pi}{2b_2}(a_2-x)\right] \cos\frac{n\pi y}{2b_2} & \text{for } \begin{cases} \ell \leq x \leq a_2 \\ 0 \leq y \leq b_2 \end{cases} \end{cases} \tag{51b}$$

and

$$\begin{cases} H_x = -\sqrt{\frac{\epsilon}{\mu_0}} E_y \\ H_y = \sqrt{\frac{\epsilon}{\mu_0}} H_x \end{cases} \tag{52}$$

Here we tabulated only the fields in one-quarter of the region in the TEM line, fields in the other three regions can also be found in a similar fashion.

VI. DETERMINING THE COUPLING COEFFICIENTS.

Let us now introduce slots to the common wall between the coaxial line and the beam-guide. These slots are intorduced so that the field configuration in the main beam guide is not significantly altered because of the presence of the scattered slot field. This is equivalent to saying that the perturbation due to the slot is small compared with the normal operation in the absence of the slot. If this is true, one can determine the wave number (Γ) of the beam current (and consequently the associated fields) and the amplitude of voltage V_o on the center conductor of the coaxial line by requiring that the total electric flux and tangential component of the magnetic field be continuous across the slot. Bearing in mind that potential and field equations in the coaxial line are referring to their own coordinate system, thus when it comes to matching the boundary conditions, appropriate values must be set for the coordinate systems on both sides of the boundaries. For instance, in the case of total electric flux flows across the boundary, we must have

$$\int_S \epsilon_c E_{cy}(x, 0, z)\, dx\, dz = \int_S \epsilon_g E_{gy}(x, b, z)\, dx\, dz \tag{53}$$

where the subscript c and g are referring to the coaxial line and the beam guide, respectively, and S is the surface area of the slot. Without loss of generality, let us assume that the slot is displaced x_3 toward the right from the center of the coax and from the beam guide. Using Eq. (53) we see that

$$-\epsilon \int_{-z_3/2}^{z_3/2} dz \int_{-(a_3-x_3)}^{-\ell} dx \sum_{n=odd}^{2N-1} B_n \sinh\left[\frac{n\pi}{2b_2}(a_2+x)\right] \frac{n\pi}{2b_2} e^{-jkz}$$

$$-\epsilon \int_{-z_3/2}^{z_3/2} dz \int_{-\ell}^{\ell} dx \left[\sum_{m=1}^{\infty} A_m \cosh\left(\frac{m\pi x}{c_2}\right)\left(\frac{m\pi}{c_2}\right) + \left(\frac{V_o}{c_2}\right)\right] e^{-jkz}$$

$$-\epsilon \int_{-z_3/2}^{z_3/2} dz \int_{\ell}^{x_3+a_3} dx \sum_{n=odd}^{2N-1} B_n \sinh\left[\frac{n\pi}{2b_2}(a_2-x)\right] \frac{n\pi}{2b_2} e^{-jkz}$$

$$= \frac{-\Gamma}{\omega\epsilon_o} \epsilon_o \int_{\frac{a}{2}-a_3+x_3}^{\frac{a}{2}+x_3+a_3} dx \int_{-z_3/2}^{z_3/2} dz \sum_{m,n} \frac{J_{mn}\, n\pi}{(\Gamma^2 - \Gamma_{mn}'^2)b} \left[\sin\left(\frac{m\pi x}{a}\right)(-1)^n\right] e^{-j\Gamma z} \tag{54}$$

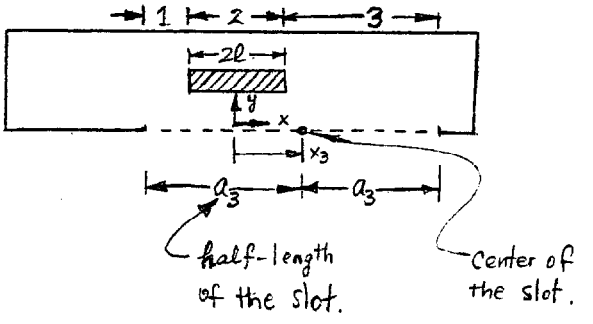

Fig 5. Slot location relative to the TEM line.

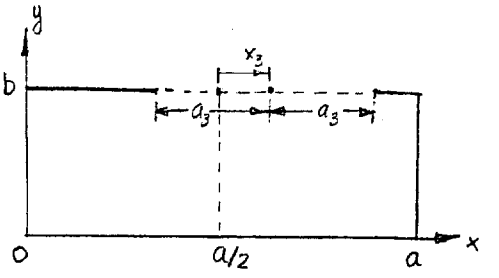

Fig 6. Slot location relative to the beam chamber.

Note that in Eq. (54), we have assumed that the slot is located at z = o and and it has a width z_3 and the electric field vector $\vec{E} = -\nabla\phi$. Integrations on the left hand side of Eq. (54) corresponds to regions 1, 2, and 3 in Figure 5 and they are non-zer0 only if the slot exists in that particular region. The dielectric constants in the coax and in the beam guide are also assumed to be ϵ and ϵ_0 respectively. Evaluting the integrations in Eq. (54), it becomes

$$\epsilon \sum_{n=odd}^{2N-1} B_n \left[\cosh\frac{n\pi}{2b_2}(a_2-\ell) - \cosh\frac{n\pi}{2b_2}(a_2+x_3-a_3)\right] \frac{2\sin(kz_3/2)}{k}$$

$$+\epsilon\left\{\sum_{m=1}^{\infty} A_m\left[\sinh\frac{m\pi}{c_2}\ell - \sinh\frac{m\pi}{c_2}(-\ell)\right] + \frac{2\ell V_0}{c_2}\right\}\frac{2\sin(kz_3/2)}{k}$$

$$-\epsilon\sum_{n=odd}^{2N-1} B_n\left[\cosh\frac{n\pi}{2b_2}(a_2-x_3-a_3) - \cosh\frac{n\pi}{2b_2}(a_2-\ell)\right]\frac{2\sin(kz_3/2)}{k}$$

$$=\sum_{mn}\frac{J_{mn}n\Gamma}{(\Gamma^2-\Gamma_{mn}'^2)b}\frac{\epsilon a)(-1)^n}{m\omega}\left[\cos\frac{m\pi}{a}\left(\frac{a}{2}+a_3+x_3\right)-\cos\frac{m\pi}{a}\left(\frac{a}{2}-a_3+x_3\right)\right]\frac{2\sin(\Gamma z_3/2)}{\Gamma} \qquad (55)$$

Similarly, the tangential magnetic field (H_x) are continuous across the slot boundary between the coaxial line and beam guide. Note that, for TEM coaxial line

$$\vec{H} = \sqrt{\frac{\epsilon}{\mu_0}}\,\hat{z}\times\vec{E} \qquad (56)$$

Thus, combining Eq. (56), (22c), (36) and (37), we have

$$\sqrt{\frac{\epsilon}{\mu_0}}\left[\sum_{n=odd}^{2N-1} B_n\frac{n\pi}{2b_2}\sinh\left[\frac{n\pi}{2b_2}(a_2-|x|)\right]e^{-jkz} + \sqrt{\frac{\epsilon}{\mu_0}}\left[\sum_{m=1}^{\infty} A_m\cosh\left(\frac{m\pi x}{c_2}\right)\left(\frac{m\pi}{c_2}\right)+\frac{V_0}{c_2}\right]e^{-jkz}\right.$$

$$=\sum_{mn}\frac{J_{mn}n\pi}{(\Gamma^2-\Gamma_{mn}'^2)b}\left[\sin\left(\frac{m\pi x}{a}\right)(-1)^n\right]e^{-j\Gamma z} \qquad (57)$$

Values (x, z) are evaluated in the slot only.

Integrating equation (57) over the slot area as we did above and taking the ratio of this result to (55), it is found that

$$\Gamma = k = \omega\sqrt{\mu_0 \epsilon} = \omega\sqrt{\mu_0 \epsilon_0 \epsilon_r} \tag{58}$$

which is not a surprising result. Two waves propagating in separated regions with common-hole coupling must have the same phase velocity. Otherwise, they will cancel each other and there will be no field at all.

Substituting Eq. (58) back into Eq. (55), we obtain

$$V_o = \frac{c_2}{2\ell}\left\{ -\sum_{mn} \frac{J_{mn}\, n(-1)^n a}{(k^2 - \Gamma'^2_{mn})mb}\sqrt{\frac{\mu_0}{\epsilon}}\left[\cos\frac{m\pi}{a}\left(\frac{a}{2}+a_3+x_3\right) - \cos\frac{m\pi}{a}\left(\frac{a}{2}-a_3+x_3\right)\right]\right.$$

$$-\sum_{m=1}^{\infty} 2A_m \cosh\frac{m\pi\ell}{c_2} - \sum_{n=\text{odd}}^{2N-1} B_n\left[2\cosh\frac{n\pi}{2b_2}(a_2-\ell) - \cosh\frac{n\pi}{2b_2}(a_2+x_3-a_3)\right. \tag{59}$$

$$\left.\left. - \cosh\frac{n\pi}{2b_2}(a_2-x_3-a_3)\right]\right\}$$

substituting A_m and B_n from Eqs. (47a) and (47b) into Eq. (59), we obtain an equation involves V_o alone,

$$V_o = \frac{-c_2}{2\ell}\sum_{mn}\frac{J_{mn}(-1)^n}{(k^2-\Gamma'^2_{mn})}\left(\frac{n}{m}\right)\left(\frac{a}{b}\right)\sqrt{\frac{\mu_0}{\epsilon}}\left[\cos\frac{m\pi}{a}\left(\frac{a}{2}+a_3+x_3\right) - \cos\frac{m\pi}{a}\left(\frac{a}{2}-a_3+x_3\right)\right]$$

$$-\sum_{m=1}^{\infty} 2\cosh\left(\frac{m\pi\ell}{c_2}\right)\frac{c_2}{2\ell}\,\text{Sech}\frac{m\pi\ell}{c_2}\,\frac{V_o}{\pi}(-1)^m\left\{\frac{2}{m} - \sum_{n=\text{odd}}^{2N-1}\frac{\left[n^2-\left(\frac{2b_2}{c_2}\right)^2\right]4\left(\frac{b_2}{c_2}\right)m}{\left[n^2-\left(\frac{2b_2}{c_2}\right)^2 m^2\right]N\left\{n\coth\left(\frac{\pi\ell}{c_2}\right)\coth\left[\frac{n\pi}{2b_2}(a_2-\ell)+\left(\frac{2b}{c}\right.\right.\right.}\right.$$

$$-\frac{c_2}{2\ell}\sum_{n=\text{odd}}^{2N-1}\frac{-V_o\left[n^2-\left(\frac{2b_2}{c_2}\right)^2\right]\left[2\cosh\frac{n\pi}{2b_2}(a_2-\ell)-\cosh\frac{n\pi}{2b_2}(a_2+x_3-a_3)-\cosh\frac{n\pi}{2b_2}(a_2-x_3-a_3)\right]}{N\left(\frac{2b_2}{c_2}\right)\sin\left(\frac{n\pi c_2}{2b_2}\right)\left\{n\coth\left(\frac{\pi\ell}{c_2}\right)\cosh\left[\frac{n\pi}{2b_2}(a_2-\ell)\right]+\frac{2b_2}{c_2}\sinh\left[\frac{n\pi}{2b_2}(a_2-\ell)\right]\right\}}$$

or

$$V_o = \frac{-\frac{C_2}{2\ell}\sum_{m=1} \frac{J_{mn}(-1)^n}{(k^2 - \beta_{mn}^2)}\left(\frac{n}{m}\right)\left(\frac{a}{b}\right)\sqrt{\frac{\mu_0}{\epsilon}}\left[\cos\frac{m\pi}{a}\left(\frac{a}{2}+a_3+x_3\right) - \cos\frac{m\pi}{a}\left(\frac{a}{2}-a_3+x_3\right)\right]}{1+H} \quad (60$$

where

$$H = \sum_{m=1}^{\infty} \frac{C_2}{\ell}\frac{(-1)^m}{\pi}\left\{\frac{2}{m} - \sum_{n=\text{odd}}^{2N-1} \frac{\left[n^2 - \left(\frac{2b_2}{C_2}\right)^2\right] 4\left(\frac{b_2}{C_2}\right)m}{\left[n^2 - \left(\frac{2b_2}{C_2}\right)^2 m^2\right] N\left[n\coth\left(\frac{\pi\ell}{C_2}\right)\coth\left(\frac{n\pi}{2b_2}\right)(a_2-\ell) + \left(\frac{2b_2}{C_2}\right)\right]}\right\}$$

$$- \frac{C_2}{2\ell}\sum_{n=\text{odd}}^{2N-1} \frac{\left[n^2 - \left(\frac{2b_2}{C_2}\right)^2\right]\left\{2 - \left[\frac{e^{-\frac{n\pi}{2b_2}(a_3-x_3-\ell)} + e^{-\frac{n\pi}{2b_2}(2a_2+x_3-a_3-\ell)}}{1+e^{-\frac{n\pi}{b_2}(a_2-\ell)}}\right] - \left[\frac{e^{-\frac{n\pi}{2b_2}(a_3+x_3-\ell)} + e^{-\frac{n\pi}{2b_2}(2a_2-x_3-a_3-\ell)}}{1+e^{-\frac{n\pi}{b_2}(a_2-\ell)}}\right]\right\}}{N\left(\frac{2b_2}{C_2}\right)\sin\left(\frac{n\pi C_2}{2b_2}\right)\left\{n\coth\left(\frac{\pi\ell}{C_2}\right) + \left(\frac{2b_2}{C_2}\right)\tanh\left[\frac{n\pi}{2b_2}(a_2-\ell)\right]\right\}} \quad (61$$

Eq. (60) gives the voltage on the center conductor of the coaxial line for a given geometry of main beam guide and a given beam current. Thus, it corresponds to a power coupling factor, in fact, it is a square root of the power coupling factor that Faltin [3] was looking for. It is interesting to note that this coupling value does not depend on the width, z_3, of the slot. However, this apparent paradox can be easily explained as follows: In the course of this derivation, our assumption was that a small coupling prevailed and the boundary condition was matched in such a fashion that all the electric fluxes going out of main beam guide through the slots into TEM line were completely gone into the coax. Thus, it is plausible that this tightly coupled power is completely coupled through and does not matter what size the hole is. It is shown in Eq. (55) that waves in these two systems are coupled with exactly the same velocity, thus the z dependent factor, or the width of the slot, is cancelled out on both sides of the equation. This is certainly not true in real cases. Proton (or electron) beam with high energy entering a cavity will interact with such system, protons will slow down, bunch up, give up energy in the form of wave radiation into the system, and in some cases will create an instability problem [10, 11]. In fact, this interaction is the basic operating principle between electrons and its surrounding (helix) circuits in Travelling Wave Tubes.

In order to investigate the power coupling and its transfer function between the beam guide and the TEM line, we shall use a classical approximation method [12]. If the dimensions of the slots are small compared with wavelength, the effect of the slots to the system is equivalent to an ideal electric and a magnetic dipole moment located at the center of the slot with the slot closed, hence

$$\begin{cases} \vec{P} = -\alpha_e \epsilon_0 (\hat{n}\cdot\vec{E})\hat{n} \\ \vec{M} = -\alpha_m \vec{H}_t \end{cases} \tag{62a}$$

where $\hat{n}$ is the unit normal to the plane containing the slot and α_e and α_m are polarizabilities for the electric and magnetic dipole moment in the slot and $\vec{E}$ and $\vec{H}_t$ are EM fields at the center of the slot. It was shown [13,14] that for a rectangular slot with dimensions shown

$$\begin{cases} \alpha_e = \frac{-\pi}{8} a_3 z_3^2 \\ \alpha_m = 0.864\, a_3^2 z_3 + 0.352\, a_3^3 \end{cases} \tag{62b}$$

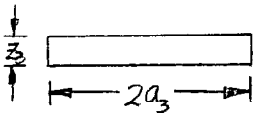

Fig. 7. Dimensions of the slot

The fields at the aperture of the slot due to the beam guide are, (see Eq. (22))

$$\begin{cases} E_y(x,b) = \frac{-k}{\omega\epsilon_0} \sum_{mn} \frac{J_{mn}\, n\pi (-1)^n}{(k^2 - \Gamma'^2_{mn})\, b} \sin\left(\frac{m\pi x}{a}\right) \\ H_x(x,b) = \sum_{m,n} \frac{J_{mn}\, n\pi (-1)^n}{(k^2 - \Gamma'^2_{mn})\, b} \sin\left(\frac{m\pi x}{a}\right) \end{cases}$$

Thus, the equivalent dipole moments for radiation into the TEM line are

$$\begin{cases} \vec{P} = -\left(\frac{k}{\omega\epsilon_0}\right)\cdot\left(\frac{\pi}{8} a_3 z_3^2\right)\epsilon_0 \sum_{mn} \frac{J_{mn}\, n\pi (-1)^n}{(k^2 - \Gamma'^2_{mn})\, b} \sin\left[\frac{m\pi(\frac{a}{2}+x_3)}{a}\right]\hat{y} \\ \vec{M} = -(0.864\, a_3^2 z_3 + 0.352\, a_3^3) \sum_{mn} \frac{J_{mn}\, n\pi (-1)^n}{(k^2 - \Gamma'^2_{mn})\, b} \sin\left[\frac{m\pi(\frac{a}{2}+x_3)}{a}\right]\hat{x} \end{cases} \tag{63}$$

Let the fields in the coax radiated by the electric dipole be

$$\vec{E}^{\pm}_{ec} = \begin{cases} e_1 \vec{E}_c^{+} \\ e_2 \vec{E}_c^{-} \end{cases}, \qquad \vec{H}^{\pm}_{ec} = \begin{cases} e_1 \vec{H}_c^{+} & \text{for } z>0 \\ e_2 \vec{H}_c^{-} & \text{for } z<0 \end{cases} \tag{64a}$$

and that radiated by the magnetic dipole be

$$\vec{E}^{\pm}_{mc} = \begin{cases} e_3 \vec{E}_c^{+} \\ e_4 \vec{E}_c^{-} \end{cases}, \qquad \vec{H}^{\pm}_{mc} = \begin{cases} e_3 \vec{H}_c^{+} & \text{for } z>0 \\ e_4 \vec{H}_c^{-} & \text{for } z<0 \end{cases} \tag{64b}$$

Since there is only one mode in a TEM line, which is the transverse mode, it can be shown that [12]

$$e_1 = e_2 = -\frac{j\omega}{2P}\, \vec{P}\cdot\vec{E}_c^{-}$$

$$= -\frac{j\omega}{2P}\,\frac{k}{\omega\epsilon_0}\,\frac{\pi}{\ell}\,a_3 Z_3^2 \epsilon_0 \sum_{mn} \frac{J_{mn}\, n\pi\,(-1)^n}{(k^2 - \Gamma'^2_{mn})b} \sin\left[\frac{m\pi\left(\frac{a}{2}+x_3\right)}{a}\right]$$

$$\cdot \begin{cases} \sum_{m=1}^{\infty} A_m \frac{m\pi}{c_2} \cosh\frac{m\pi x_3}{c_2} + \frac{V_0}{c_2} & \text{for } x_3 \le \ell \\ \sum_{n=\text{odd}}^{2N-1} B_n \frac{n\pi}{2b_2} \sinh\left[\frac{n\pi}{2b_2}(a_2 - x_3)\right] & \text{for } x_3 \ge \ell \end{cases} \tag{65}$$

where $P = \int_S (\vec{E}_c \times \vec{H}_c)\cdot \hat{Z}\ ds$ = power flow in a cross sectional region of the coax

S = cross sectional region in question and the subscript g, c are referred to the beam guide and the coaxial line, respectively.

The field radiated by the magnetic dipole is

$$e_3 = -e_4 = \frac{j\omega\mu_0}{2P}\, \vec{H}_c^{-}\cdot\vec{M}$$

$$= \frac{-j\omega\mu_0}{2P}\sqrt{\frac{\epsilon}{\mu_0}}\left(0.864\,a_3^2 Z_3 + 0.352\,a_3^3\right)\sum_{mn}\frac{J_{mn}\,n\pi\,(-1)^n}{(k^2-\Gamma_{mn}'^2)\,b}\sin\left[\frac{m\pi(\frac{a}{2}+x_3)}{a}\right]$$

$$\cdot\begin{cases}\sum_{m=1}^{\infty} A_m\frac{m\pi}{c_2}\cosh\left(\frac{m\pi x_3}{c_3}\right) + V_0/c_2 & \text{for } x_3 \le \ell \\ \sum_{n=odd}^{2N-1} B_n\frac{n\pi}{2b_2}\sinh\left[\frac{n\pi}{2b_2}(a_2-x_3)\right] & \text{for } x_3 \ge \ell\end{cases} \tag{66}$$

Thus, the total EM fields in the TEM line under this dipole moment consideration is

$$\vec{E}_{TC}^{\pm} = \begin{cases}(e_1+e_3)\,\vec{E}_c^{+} \\ (e_2+e_4)\,\vec{E}_c^{-}\end{cases} = \begin{cases}(e_1+e_3)\,\vec{E}_c^{+} \\ (e_1-e_3)\,\vec{E}_c^{-}\end{cases} \tag{67}$$

and

$$\vec{H}_{TC}^{\pm} = \begin{cases}(e_1+e_3)\,\vec{H}_c^{+} \\ (e_2+e_4)\,\vec{H}_c^{-}\end{cases} = \begin{cases}(e_1+e_3)\,\vec{H}_c^{+} \\ (e_1-e_3)\,\vec{H}_c^{-}\end{cases} \tag{68}$$

where

$$\vec{E}_c^{+} = (\vec{e}_x + \vec{e}_y + \cancel{\vec{e}_z}^{\,0})\,e^{-jkz}$$

$$\vec{E}_c^{-} = (\vec{e}_x + \vec{e}_y - \cancel{\vec{e}_z}^{\,0})\,e^{jkz}$$

$$\vec{H}_c^{+} = (\vec{h}_x + \vec{h}_y + \cancel{\vec{h}_z}^{\,0})\,e^{-jkz}$$

$$\vec{H}_c^{-} = (-\vec{h}_x - \vec{h}_y + \cancel{\vec{h}_z}^{\,0})\,e^{jkz}$$

It is interesting to observe in the first sight that, if

$$e_1 = e_3 \tag{69}$$

then the term involves $e_2 + e_4 = 0$, or there will be no power flow in the $-\hat{Z}$ direction. In order for Eq. (69) to be true, it is easy to see that, if

$$\sqrt{\mu_0\epsilon}\,\frac{\pi}{8}\,a_3 Z_3^2 = \sqrt{\mu_0\epsilon}\left(0.864\,a_3^2 Z_3 + 0.352\,a_3^3\right) \tag{70}$$

or $$a_3 = 0.39\,Z_3$$

which violates our assumption which stated that the length of the slot is larger than its width [13]. Hence, there will be some power flow in the $-\hat{Z}$ direction in the coax and, it is a matter of question how to minimize it. For this unwanted reverse power can only take away useful information from the forward direction power.

It is also of interest to consider the power transfer from the beam current to the coax. From Eq. (67) and (68), the total + $\hat{Z}$ direction power is

$$P_T = \int_S \vec{E}^+_{TC} \times \vec{H}^{+*}_{TC} \cdot \hat{z}\, ds$$

$$= 2\left| e_1 + e_3 \right|^2 \int_S \vec{E}^+_c \times \vec{H}^{+*}_c \quad \hat{z}\, ds \tag{71}$$

A factor of 2 is present in Eq. (71) because there are two halves in the coax, (see Figure 4)namely, region I and II in Figure 4 is one-half, regions III and IV is the other.

However

$$P = \int_S \vec{E}_c \times \vec{H}^*_c \cdot \hat{z}\, ds$$

$$= 2\left\{ \int_0^{\ell} dx \int_0^{c_2} dy + \int_{\ell+\Delta}^{a_2} dx \int_0^{b_2} dy \right\} \left[E_x H^*_y - E_y H^*_x \right]$$

$$= 2\left\{ \int_0^{\ell} dx \int_0^{c_2} dy + \int_{\ell+\Delta}^{a_2} dx \int_0^{b_2} dy \right\} \left[|E_x|^2 + |E_y|^2 \right] \sqrt{\frac{\epsilon}{\mu_0}}$$

$$= 2\sqrt{\frac{\epsilon}{\mu_0}} \left\{ \int_0^{\ell} dx \int_0^{c_2} dy \left[\sum_{m=1}^{\infty} A_m^2 \left(\frac{m\pi}{c_2}\right)^2 \sinh^2\left(\frac{m\pi x}{c_2}\right) \sin^2 \frac{m\pi y}{c_2} + \sum_{m=1}^{\infty} A_m^2 \left(\frac{m\pi}{c_2}\right)^2 \cosh^2 \frac{m\pi x}{c_2} \cos^2 \frac{m\pi y}{c_2} \right.\right.$$

$$\left.\left. + \frac{V_b^2}{c_2^2} \right]\right\} + 2\sqrt{\frac{\epsilon}{\mu_0}} \left\{ \int_{\ell+\Delta}^{a_2} dx \int_0^{b_2} dy \left[\sum_{n=odd}^{2N-1} B_n^2 \left(\frac{n\pi}{2b_2}\right)^2 \cosh^2\left[\frac{n\pi}{2b_2}(a_2 - x)\right] \sin^2\left(\frac{n\pi y}{2b_2}\right) \right.\right.$$

$$\left.\left. + \sum_{n=odd}^{2N-1} B_n^2 \left(\frac{n\pi}{2b_2}\right)^2 \sinh^2\left[\frac{n\pi}{2b_2}(a_2 - x)\right] \cos^2 \frac{n\pi y}{2b_2} \right]\right\}$$

$$= \frac{1}{2}\sqrt{\frac{\epsilon}{\mu_c}} \sum_{m=1}^{\infty} A_m^2\, m\pi \sinh\left(\frac{2m\pi\ell}{c_2}\right) + 2\sqrt{\frac{\epsilon}{\mu_r}}\,\frac{V_c^2\,\ell}{c_2}$$

$$+ \frac{1}{2}\sqrt{\frac{\epsilon}{\mu_0}} \sum_{n=odd}^{2N-1} B_n^2\, n\pi \sinh\left[\frac{2n\pi}{2b_2}(a_2-\ell)\right] \qquad (72)$$

A factor of 2 in the second step in Eq.(72) is because the slot involves 2 regions, namely, region I and II in Figure 4. A small positive value has been instroduced in the lower limit of the integrations. This is done so that slow convergence in the summation is avoided. Combining Eqs.(65) and (71), we obtain

$$P_T = 2\,|e_1 + e_3|^2\, P$$

$$= \frac{2k^2}{P}\left[0.432\,a_3^2 z_3 + 0.2244\,a_3 z_3^2 + 0.176\,a_3^3\right]\left[\sum_{mn}\frac{J_{mn}\, n\pi\,(-1)^n}{(k^2-\Gamma_{mn}'^2)\,b}\sin\frac{m\pi}{a}\left(\frac{a}{2}+x_3\right)\right]^2 \qquad (73)$$

$$\begin{cases} \sum_{m=1}^{\infty} A_m \frac{m\pi}{c_2}\cosh\frac{m\pi x_3}{c_2} + \frac{V_0}{c_2} \\ \sum_{n=odd}^{2N-1} B_n \frac{n\pi}{2b_2}\sinh\left[\frac{n\pi}{2b_2}(a_2-x_3)\right] \end{cases}^2 \quad \begin{matrix} \text{for } x_3 \le \ell \\ \text{for } x_3 \ge \ell \end{matrix}$$

Eq. (73) gives us the power in the coax for a given value of beam current in the beam chamber. This power is increased by a factor of 2 if two TEM lines, one on each broadside wall, are coupled with the beam guide. This power couple relationship can also be used to calculate the transfer function of the system, in this instance, it is a coupling resistance

$$R_T = \frac{2P_T}{I_{z0}^2}$$

$$= \frac{4k^2}{P\,I_{z0}^2}\left[0.432 a_3^2 z_3 + 0.2244\,a_3 z_3^2 + 0.176\,a_3^3\right]^2\cdot\left[\sum_{mn}\frac{J_{mn}\, n\pi\,(-1)^n}{(k^2-\Gamma_{mn}'^2)\,b}\sin\frac{m\pi}{a}\left(\frac{a}{2}+x_3\right)\right]^2$$

$$\cdot\begin{cases} \sum_{m=1}^{\infty} A_m\left(\frac{m\pi}{c_2}\right)\cosh\frac{m\pi x_3}{c_2} + V_0/c_2 \\ \sum_{n=odd}^{2N-1} B_n\left(\frac{n\pi}{2b_2}\right)\sinh\left[\frac{n\pi}{2b_2}(a_2-x_3)\right] \end{cases}^2 \quad \begin{matrix} \text{for } x_3 \le \ell \\ \text{for } x_3 > \ell \end{matrix} \qquad (74)$$

VII. MULTI-SLOT COUPLING IN THE PICKUP.

So far we have limited ourselves in the case one slot coupling in the pick-up. However, we are more interested in a pick-up with more than one hole, or a larger coupling resistance. To this end, we want to explore the effect of multihole coupling in the following. Fig. 8 gives the geometry of this coupling. A unit amplitude wave propagates in the lower guide is scattered through the slot and a very small part of the power is transmitted through the hole to become a forward and backward wave in the upper guide. The coupling coefficients A_f and A_b are referred to forward and backward coupling coefficients. They were found in the previous sections. If the coupling is small enough, the amplitude of the incident wave at the second slot down the line is essentially the same as the first slot. However, due to the difference in path length, a phase delay of e^{-jkd} is resulted. By virtual of Eq. (58), waves in the upper and lower guides are propagating with the same speed, wave amplitude at the second slot in the upper guide due to the first slot scattering is also delayed by e^{-jkd}. Hence, the total amplitude at the second slot is $2A_f e^{-jkd}$. In other words forward waves always add in phase. Thus, for N_s slot coupling, the coupling resistance is increased by a factor of N_s, i.e.

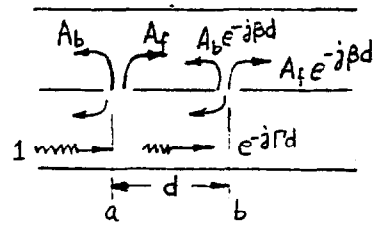

Fig. 8. Multi-slot Coupling.

$$R_{TN} = N_S R_T \tag{75a}$$

For the backward propagating power, it is easy to see that the total value for two slots is $A_b(1 + e^{-j2\beta d})$, or for N_s slots, this becomes

$$\text{Total backward wave} = A_b \left[1 + \sum_{n=2}^{N_s} e^{-j2\beta nd}\right] \tag{75b}$$

Therefore, the backward power is zero only if $d = \left(\frac{m}{4n}\right)\lambda$, where $m = 1, 3, 5, \cdots$ This is impossible for our operating frequence. In other words, there will be some backward power in the coax.

Let us now consider the ratio of power coupled into the TEM line to the total power generated by the beam current. For the case in which TM_{11} modes was excited in the beam guide, from Eq.(24), the total power generated by the beam current is

$$P_B = \frac{k\pi^2}{8\omega\epsilon_0 ab} \cdot \frac{J_{11}^2(a^2+b^2)}{\left[k^2 - \Gamma_{mn}'^2\right]^2} \tag{76}$$

and the power coupled into the TEM line, from Eq.(73), is

$$P_T = \frac{2k}{P}\left[0.432\left(\frac{z_3}{a_3}\right)+0.2244\left(\frac{z_3}{a_3}\right)^2+0.176\right]^2 \frac{a_3^6\,\pi^2\cos^2\left(\frac{\pi x_3}{a}\right)J_{11}^2}{\left(k^2-\Gamma_{mn}'^2\right)^2 b^2}\left\{\sum_{m=1}^{\infty} A_m \frac{m\pi}{c_2}\cosh\left(\frac{m\pi x_3}{c_2}\right)+\frac{V_0}{c_2}\right\}^2 \left\{\sum_{n=\text{odd}}^{2N-1} B_n \frac{n\pi}{2b_2}\sinh\left[\frac{n\pi}{2b_2}(a_2-x_3)\right]\right\}^2 \quad (7$$

Therefore,

$$\frac{P_T}{P_B} = \frac{2k\left[0.432\left(\frac{z_3}{a_3}\right)+0.2244\left(\frac{z_3}{a_3}\right)^2+0.176\right]^2\cos^2\left(\frac{\pi x_3}{a}\right)\left\{\sum_{m=1}^{\infty} A_m \frac{m\pi}{c_2}\cosh\left(\frac{m\pi x_3}{c_2}\right)+\frac{V_0}{c_2}\right\}^2 \left\{\sum_{n=\text{odd}}^{2N-1} B_n \frac{n\pi}{2b_2}\sinh\left[\frac{n\pi}{2b_2}(a_2-x_3)\right]\right\}^2 8\omega\epsilon_0 ab\,a_3^6}{P\,b^2(a^2+b^2)}$$

$$= \frac{16k\,\omega\epsilon_0 a\left[0.432\left(\frac{z_3}{a_3}\right)+0.2244\left(\frac{z_3}{a_3}\right)^2+0.176\right]^2 a_3^6\cos^2\left(\frac{\pi x_3}{a}\right)\left\{\sum_{m=1}^{\infty} A_m \frac{m\pi}{c_2}\cosh\frac{m\pi x_3}{c_2}+\frac{V_0}{c_2}\right\}^2 \left\{\sum_{n=\text{odd}}^{2N-1} B_n \frac{n\pi}{2b_2}\sinh\left[\frac{n\pi}{2b_2}(a_2-x_3)\right]\right\}^2}{P\,b(a^2+b^2)} \quad (78)$$

It is shown in Section IX that, for any reasonable dimensions in a, b, a_3, x_3 and operating frequency, Eq.(78) gives a value less than 10^{-4}. This thus verifies our earlier assumption that weak coupling between the power in the beam guide and that of the TEM line.

VIII. THE KICKER

In the kicker, we want to determine a change of momentum in the current carriers(protons) for a given input voltage V_0 in the center conductor of the TEM line, assuming a similar physical structure in the kicker as in the pick-up. In this analysis, we shall assume that the presence of the beam has no effect on the field configuration in the chamber. This assumption is justifiable if the signal fed to the beam is much greater than that of the generated by the beam and, the beam chamber is made in such a way that only dorminant modes are excited. For a given feed-forward signal V_0, the fields in the TEM line are given in Eqs.(51) and (52), with coefficients A_m and B_n given in Eq.(4). Thus, the field in the slot on the TEM line side are:

$$E_{yc}(x,0) = \begin{cases} -\sum_{m=1}^{\infty} A_m \frac{m\pi}{c_2}\cosh\frac{m\pi x}{c_2} - \frac{V_0}{c_2} & \text{for } 0 \le x \le \ell \\ -\sum_{n=\text{odd}}^{2N-1} B_n \frac{n\pi}{2b_2}\sinh\left[\frac{n\pi}{2b_2}(a_2-x)\right] & \text{for } \ell < x \le a_2 \end{cases} \quad (79a)$$

$$H_{xc}(x,0) = -\sqrt{\frac{\epsilon}{\mu_o}}\, E_{yc}(x,0) \tag{79b}$$

Thus, the equivalent dipole moments are

$$\begin{cases} \vec{P} = -\alpha_e \epsilon_o E_{yc}(x,0)\,\hat{y} = P\,\hat{y} \\ \vec{M} = -\alpha_m H_{xc}(x,0)\,\hat{x} = \alpha_m \sqrt{\frac{\epsilon}{\mu_o}}\, E_{yc}(x,0)\,\hat{x} = M\,\hat{x} \end{cases} \tag{80}$$

where α_e and α_m are given in Eq.(62) and x_3 is the center of the slot from the center toward the right hand side of the broad side wall of the TEM line or the beam chamber as we discussed in Section VI.

The waveguide fields in the beam chamber are given in Eqs. (8), (4) and (2).

$$\begin{cases} E_x^{TM}(x,y) = -\frac{\Gamma'_{mn}}{\omega\epsilon_o}\left(\frac{m\pi}{a}\right)\cos\left(\frac{m\pi x}{a}\right)\sin\left(\frac{n\pi y}{b}\right) \\ E_y^{TM}(x,y) = -\frac{\Gamma'_{mn}}{\omega\epsilon_o}\left(\frac{n\pi}{b}\right)\sin\left(\frac{m\pi x}{a}\right)\cos\left(\frac{n\pi y}{b}\right) \\ E_z^{TM}(x,y) = \frac{j(\Gamma'^2_{mn} - \beta_o^2)}{\omega\epsilon_o}\sin\left(\frac{m\pi x}{a}\right)\sin\left(\frac{n\pi y}{b}\right) \\ H_x^{TM}(x,y) = \left(\frac{n\pi}{b}\right)\sin\left(\frac{m\pi x}{a}\right)\cos\left(\frac{n\pi y}{b}\right) \\ H_y^{TM}(x,y) = -\left(\frac{m\pi}{a}\right)\cos\left(\frac{m\pi x}{a}\right)\sin\left(\frac{n\pi y}{b}\right) \end{cases} \tag{81}$$

where

$$\Gamma'^2_{mn} = \beta_o^2 - \left(\frac{m\pi}{a}\right)^2 - \left(\frac{n\pi}{b}\right)^2$$

whereas for TE waves, we have[12]:

$$
\begin{cases}
H_z^{TE}(x,y) = \cos\left(\frac{m\pi x}{a}\right)\cos\left(\frac{n\pi y}{b}\right) \\
H_x^{TE}(x,y) = \frac{\partial \Gamma_{mn}}{(\beta_0^2 - \Gamma_{mn}'^2)}\left(\frac{m\pi}{a}\right)\sin\left(\frac{m\pi x}{a}\right)\cos\left(\frac{n\pi y}{b}\right) \\
H_y^{TE}(x,y) = \frac{\partial \Gamma_{mn}'}{(\beta_0^2 - \Gamma_{mn}'^2)}\left(\frac{n\pi}{b}\right)\cos\left(\frac{m\pi x}{a}\right)\sin\left(\frac{n\pi y}{b}\right) \\
E_x^{TE}(x,y) = \frac{\partial \omega\mu_0}{(\beta_0^2 - \Gamma_{mn}'^2)}\left(\frac{n\pi}{b}\right)\cos\left(\frac{m\pi x}{a}\right)\sin\left(\frac{n\pi y}{b}\right) \\
E_y^{TE}(x,y) = \frac{-\partial \omega\mu_0}{(\beta_0^2 - \Gamma_{mn}'^2)}\left(\frac{m\pi}{a}\right)\sin\left(\frac{m\pi x}{a}\right)\cos\left(\frac{n\pi y}{b}\right)
\end{cases}
\tag{82}
$$

Fields generated by these electric and magnetic dipoles in the beam chamber can be expressed as:

$$
\begin{cases}
\vec{E}^{TM} = \sum_{mn} A_{mn}^{TM}\,\vec{E}_{mn}^{+TM} + \sum_{mn} B_{mn}^{TM}\,\vec{E}_{mn}^{-TM} \\
\vec{H}^{TM} = \sum_{mn} A_{mn}^{TM}\,\vec{H}_{mn}^{+TM} + \sum_{mn} B_{mn}^{TM}\,\vec{H}_{mn}^{-TM}
\end{cases}
\tag{83a}
$$

$$
\begin{cases}
\vec{E}^{TE} = \sum_{mn} A_{mn}^{TE}\,\vec{E}_{mn}^{+TE} + \sum_{mn} B_{mn}^{TE}\,\vec{E}_{mn}^{-TE} \\
\vec{H}^{TE} = \sum_{mn} A_{mn}^{TE}\,\vec{H}_{mn}^{+TE} + \sum_{mn} B_{mn}^{TE}\,\vec{H}_{mn}^{-TE}
\end{cases}
\tag{83b}
$$

where

$$
\begin{Bmatrix} A_{mn}^{TM} \\ B_{mn}^{TM} \end{Bmatrix} = \frac{\partial \omega}{2P_{TM}}\left(\mu_0 \vec{H}_{mn}^{\mp TM}\cdot\vec{M} - \vec{E}_{mn}^{\mp TM}\cdot\vec{P}\right) \tag{84a}
$$

similarly

$$
\begin{Bmatrix} A_{mn}^{TE} \\ B_{mn}^{TE} \end{Bmatrix} = \frac{\partial \omega}{2P_{TE}}\left(\mu_0 \vec{H}_{mn}^{\mp TE}\cdot\vec{M} - \vec{E}_{mn}^{\mp TE}\cdot\vec{P}\right) \tag{84b}
$$

If only dominant TE or TM modes are to be excited in the beam chamber, i.e. TE_{10} and TM_{11} modes only, the corresponding field equations are

$$\begin{cases} E_x^{TM} = -\frac{\Gamma_{11}'}{\omega\epsilon_o}\left(\frac{\pi}{a}\right)\cos\left(\frac{\pi x}{a}\right)\sin\left(\frac{\pi y}{b}\right) \\ E_y^{TM} = -\frac{\Gamma_{11}'}{\omega\epsilon_o}\left(\frac{\pi}{b}\right)\sin\left(\frac{\pi x}{a}\right)\cos\left(\frac{\pi y}{b}\right) \\ E_z^{TM} = \frac{j(\Gamma_{11}'^2 - \beta_o^2)}{\omega\epsilon_o}\sin\left(\frac{\pi x}{a}\right)\sin\left(\frac{\pi y}{b}\right) \\ H_x^{TM} = \left(\frac{\pi}{b}\right)\sin\left(\frac{\pi x}{a}\right)\cos\left(\frac{\pi y}{b}\right) \\ H_y^{TM} = -\left(\frac{\pi}{a}\right)\cos\left(\frac{\pi x}{a}\right)\sin\left(\frac{\pi y}{b}\right) \end{cases} \tag{85a}$$

while for TE_{10} case

$$\begin{cases} H_z^{TE} = \cos\left(\frac{\pi x}{a}\right) \\ H_x^{TE} = \frac{j\Gamma_{10}' a}{\pi}\sin\left(\frac{\pi x}{a}\right) \\ E_y^{TE} = \frac{-j\omega\mu_o a}{\pi}\sin\left(\frac{\pi x}{a}\right) \end{cases} \tag{85b}$$

Thus, from Eq. (81a), we have

$$A_{11}^{TM} = \frac{j\omega}{2P_{TM}}\left[\mu_o\left(\frac{\pi}{b}\right)\sin\frac{\pi\left(\frac{a}{2}+x_3\right)}{a}\cdot M - \frac{\Gamma_{11}'}{\omega\epsilon_o}\left(\frac{\pi}{b}\right)\sin\frac{\pi\left(\frac{a}{2}+x_3\right)}{a}\cdot P\right]$$

$$= \frac{j\omega}{2P_{TM}}\left(\frac{\pi}{b}\right)\cos\left(\frac{\pi x_3}{a}\right)\left[\mu_o M - \frac{\Gamma_{11}'}{\omega\epsilon_o}P\right]$$

$$= \frac{j\omega}{2P_{TM}}\left(\frac{\pi}{b}\right)\cos\left(\frac{\pi x_3}{a}\right)\left[\mu_o\alpha_m\sqrt{\frac{\epsilon}{\mu_o}} - |\alpha_e|\epsilon_o\frac{\Gamma_{11}'}{\omega\epsilon_o}\right]E_{yc}(x_3, 0)$$

$$= \frac{j\omega}{2P_{TM}}\left(\frac{\pi}{b}\right)\cos\left(\frac{\pi x_3}{a}\right)\left[\alpha_m\sqrt{\mu_o\epsilon} - |\alpha_e|\frac{\Gamma_{11}'}{\omega}\right]E_{yc}(x_3, 0)$$

where

$$P_{TM} = \int_0^a dx \int_0^b dy \left(E_x^{TM} H_y^{TM} - E_y^{TM} H_x^{TM} \right)$$

$$= \frac{\Gamma_{11}'}{\omega \epsilon_o} \int_0^a dx \int_0^b dy \left[\left(\frac{\pi}{a}\right)^2 \cos^2\left(\frac{\pi x}{a}\right) \sin^2\left(\frac{\pi y}{b}\right) + \left(\frac{\pi}{b}\right)^2 \sin^2\left(\frac{\pi x}{a}\right) \cos^2\left(\frac{\pi y}{b}\right) \right]$$

$$= \frac{\Gamma_{11}'}{4 \omega \epsilon_o} \left[\frac{a^2 + b^2}{ab} \right] \tag{86}$$

or

$$A_{11}^{TM} = \frac{2 j \omega^2 \epsilon_o}{\Gamma_{11}' \pi} \left(\frac{a}{a^2+b^2} \right) \cos\left(\frac{\pi x_3}{a}\right) \left[\alpha_m \sqrt{\mu_o \epsilon} - |\alpha_e| \frac{\Gamma_{11}'}{\omega} \right] E_{yc}(x_3, 0) \tag{87a}$$

similarly

$$B_{11}^{TM} = \frac{j\omega}{2 P_{TM}} \left[-\mu_o \left(\frac{\pi}{b}\right) \sin \frac{\pi\left(\frac{a}{2}+x_3\right)}{a} \cdot M + \frac{\Gamma_{11}'}{\omega \epsilon_o} \left(\frac{\pi}{b}\right) \sin \frac{\pi\left(\frac{a}{2}+x_3\right)}{a} \cdot P \right]$$

$$= \frac{-2 j \omega^2 \epsilon_o}{\Gamma_{11}' \pi} \left(\frac{a}{a^2+b^2} \right) \cos \frac{\pi x_3}{a} \left[\alpha_m \sqrt{\mu_o \epsilon} + |\alpha_e| \frac{\Gamma_{11}'}{\omega} \right] E_{yc}(x_3, 0) \tag{87b}$$

and

$$A_{10}^{TE} = \frac{j\omega}{2 P_{TE}} \left[\mu_o \cdot \frac{j \Gamma_{10}' a}{\pi} \sin \frac{\pi\left(\frac{a}{2}+x_3\right)}{a} \cdot M + \frac{j \omega \mu_o a}{\pi} \sin \frac{\pi\left(\frac{a}{2}+x_3\right)}{a} \cdot P \right]$$

$$= \frac{\omega \mu_o}{2 P_{TE}} \left(\frac{a}{\pi} \right) \cos\left(\frac{\pi x_3}{a}\right) \left[\Gamma_{10}' M - \omega P \right]$$

$$= \frac{\omega \mu_o}{2 P_{TE}} \left(\frac{a}{\pi} \right) \cos\left(\frac{\pi x_3}{a}\right) \left[\Gamma_{10}' \alpha_m \sqrt{\frac{\epsilon}{\mu_o}} - |\alpha_e| \omega \epsilon_o \right] E_{yc}(x_3, 0)$$

with

$$P_{TE} = \int_0^a dx \int_0^b dy \; -E_y^{TE} H_x^{TE}$$

$$= -\omega \mu_o \Gamma_{10}' \left(\frac{a}{\pi}\right)^2 \frac{ab}{2}$$

or

$$A_{10}^{TE} = -\frac{\pi}{\Gamma_{10}' a^2 b} \cos\frac{\pi x_3}{a} \left[\Gamma_{10}' \alpha_m \sqrt{\frac{\epsilon}{\mu_o}} - \omega |\alpha_e| \epsilon_o \right] E_{yc}(x_3, 0) \qquad (88a)$$

Similarly,

$$B_{10}^{TE} = \frac{\pi}{\Gamma_{10}' a^2 b} \cos\frac{\pi x_3}{a} \left[\Gamma_{10}' \alpha_m \sqrt{\frac{\epsilon}{\mu_o}} + \omega |\alpha_e| \epsilon_o \right] E_{yc}(x_3, 0) \qquad (88b)$$

Hence the total electric and magnetic fields inside the beam chamber that are affecting the beam current are:

$$\vec{E}(x,y,z) = A_{11}^{TM} \vec{E}_{11}^{+TM} + B_{11}^{TM} \vec{E}_{11}^{-TM} + A_{10}^{TE} \vec{E}_{10}^{+TE} + B_{10}^{TE} \vec{E}_{10}^{-TE}$$

$$= \frac{2j\omega^2\epsilon_o}{\Gamma_{11}' \pi} \left(\frac{a}{a^2+b^2}\right) \cos\left(\frac{\pi x_3}{a}\right) \left[\alpha_m \sqrt{\mu_o \epsilon} - |\alpha_e| \frac{\Gamma_{11}'}{\omega} \right] E_{yc}(x_3, 0) \left[\hat{x} E_{x11}^{TM} + \hat{y} E_{y11}^{TM} + \hat{z} E_{z11}^{TM} \right] e^{-j\Gamma_{11}' z}$$

$$- \frac{2j\omega^2\epsilon_o}{\Gamma_{11}' \pi} \left(\frac{a}{a^2+b^2}\right) \cos\left(\frac{\pi x_3}{a}\right) \left[\alpha_m \sqrt{\mu_o \epsilon} + |\alpha_e| \frac{\Gamma_{11}'}{\omega} \right] E_{yc}(x_3, 0) \left[\hat{x} E_{x11}^{TM} + \hat{y} E_{y11}^{TM} - \hat{z} E_{z11}^{TM} \right] e^{j\Gamma_{11}' z}$$

$$- \frac{\pi}{\Gamma_{10}' a^2 b} \cos\left(\frac{\pi x_3}{a}\right) \left[\Gamma_{10}' \alpha_m \sqrt{\frac{\epsilon}{\mu_o}} - \omega |\alpha_e| \epsilon_o \right] E_{yc}(x_3, 0) \left[\hat{y} E_{y10}^{TE} \right] e^{-j\Gamma_{10}' z}$$

$$+ \frac{\pi}{\Gamma_{10}' a^2 b} \cos\left(\frac{\pi x_3}{a}\right) \left[\Gamma_{10}' \alpha_m \sqrt{\frac{\epsilon}{\mu_o}} + \omega |\alpha_e| \epsilon_o \right] E_{yc}(x_3, 0) \left[\hat{y} E_{y10}^{TE} \right] e^{j\Gamma_{10}' z} \qquad (89a)$$

similarly, from Eq. (80)

$$\vec{H}(x,y,z) = A_{11}^{TM} \vec{H}_{11}^{+TM} + B_{11}^{TM} \vec{H}_{11}^{-TM} + A_{10}^{TE} \vec{H}_{10}^{+TE} + B_{10}^{TE} \vec{H}_{10}^{-TE}$$

$$= \frac{2j\omega^2\epsilon_o}{\Gamma_{11}' \pi} \left(\frac{a}{a^2+b^2}\right) \cos\left(\frac{\pi x_3}{a}\right) \left[\alpha_m \sqrt{\mu_o \epsilon} - |\alpha_e| \frac{\Gamma_{11}'}{\omega} \right] E_{yc}(x_3, 0) \left[\hat{x} H_{x11}^{TM} + \hat{y} H_{y11}^{TM} \right] e^{-j\Gamma_{11}' z}$$

$$- \frac{2j\omega^2\epsilon_o}{\Gamma_{11}'\pi}\left(\frac{a}{a^2+b^2}\right)\cos\left(\frac{\pi x_3}{a}\right)\left[\alpha_m\sqrt{\mu_o\epsilon} + |\alpha_e|\frac{\Gamma_{11}'}{\omega}\right]E_{yc}(x_3,0)\left[-\hat{x}\,H_{x11}^{TM} - \hat{y}\,H_{y11}^{TM}\right]e^{j\Gamma_{11}'z}$$

$$-\frac{\pi}{\Gamma_{10}'a^2b}\cos\left(\frac{\pi x_3}{a}\right)\left[\Gamma_{10}'\alpha_m\sqrt{\frac{\epsilon}{\mu_o}} - \omega|\alpha_e|\epsilon_o\right]E_{yc}(x_3,0)\left[\hat{x}\,H_{x10}^{TE} + \hat{z}\,H_{z10}^{TE}\right]e^{-j\Gamma_{10}'z}$$

$$+\frac{\pi}{\Gamma_{10}'a^2b}\cos\left(\frac{\pi x_3}{a}\right)\left[\Gamma_{10}'\alpha_m\sqrt{\frac{\epsilon}{\mu_o}} + \omega|\alpha_e|\epsilon_o\right]E_{yc}(x_3,0)\left[-\hat{x}\,H_{x10}^{TE} + \hat{z}\,H_{z10}^{TE}\right]e^{j\Gamma_{10}'z} \quad (89b$$

where E_{11}^{TM}, H_{11}^{TM}, E_{10}^{TE}, and H_{10}^{TE} are given in Eq.(82a) and (82b)

In fact in the case of a beam chamber with a = 15.5 cm and b = 7.5 cm, and operating at 1 GHz frequency, only TE_{10} mode can propagate in this waveguide. Thus, only TE_{10} waves are involved in Eq. (86). In that case, we can also determine the size of the slot such that $A_{10}^{TE} = 0$, or

$$\Gamma_{10}'\alpha_m\sqrt{\frac{\epsilon}{\mu_o}} - \omega|\alpha_e|\epsilon_o = 0 \quad (90)$$

In view of Eq. (62b), we see that

$$\Gamma_{10}'\sqrt{\frac{\epsilon}{\mu_o}}\left(0.864\,a_3z_3 + 0.352\,a_3^2\right) - \omega\epsilon_o\frac{\pi}{8}z_3^2 = 0$$

or

$$a_3 = 3z_3 \quad (91)$$

For this special case, we have

$$\vec{E}(x,y,z) = B_{10}^{TE}\vec{E}_{10}^{-TE} = \frac{-2\pi}{\Gamma_{10}'a^2b}\cos\left(\frac{\pi x_3}{a}\right)\Gamma_{10}'\alpha_m\sqrt{\frac{\epsilon}{\mu_o}}E_{yc}(x_3,0)\frac{j\omega\mu_o a}{\pi}\sin\left(\frac{\pi x}{a}\right)e^{j\Gamma_{10}'z}\hat{y}$$

$$= \frac{-2j\omega\sqrt{\mu_o\epsilon}\,\alpha_m}{ab}\cos\left(\frac{\pi x_3}{a}\right)E_{yc}(x_3,0)\sin\left(\frac{\pi x}{a}\right)e^{j\Gamma_{10}'z}\hat{y} \quad (92a)$$

and $$\vec{H}(x,y,z) = B_{10}^{TE}\,\vec{H}_{10}^{TE}$$

$$= \frac{2\pi}{a^2 b}\,\alpha_m\sqrt{\frac{\epsilon}{\mu_0}}\cos\left(\frac{\pi x_3}{a}\right) E_{yc}(x_3,0)\left[-\hat{x}\,j\,\frac{\Gamma'_{10}a}{\pi}\sin\left(\frac{\pi x}{a}\right) + \hat{z}\cos\left(\frac{\pi x}{a}\right)\right]\cdot e^{j\Gamma' z} \qquad (92b)$$

The momentum of the carriers under the influence of these electromagnetic fields is

$$\frac{d\vec{P}}{dt} = q(\vec{E} + \vec{v}\times\mu_0\vec{H})$$

or a change of momentum

$$\Delta\vec{P} = \vec{P} - \vec{P}_0 = q\int_0^{t_1}(\vec{E} + \vec{v}\times\mu_0\vec{H})\,dt \qquad (93)$$

Although Eq. (93) can be solved exactly for the given expressions for $\vec{E}$ and $\vec{H}$ in Eq. (92)[15], we shall make a simple assumption that the position of the particles does not change siginificantly after each kick, thus the integral in Eq. (93) is assumed to be constant. The time t, is the time interval particles under active influence by a slot.

$$\Delta\vec{P} = q\int_0^{t_1}\left[E_y\hat{y} + \mu_0 v\hat{z}\times(\hat{x}H_x + \hat{z}H_z)\right]e^{j\omega t}\,dt$$

$$\simeq \hat{y}\,q\left[E_y + \mu_0 v H_x\right]\cdot\left(e^{j\omega t_1} - 1\right)/j\omega$$

$$= -\hat{y}\,2q\sqrt{\mu_0\epsilon}\,\alpha_m\cdot\frac{1}{ab}\cdot\cos\left(\frac{\pi x_3}{a}\right)E_{yc}(x_3,0)\sin\left(\frac{\pi x}{a}\right)$$

$$\left(1 + \frac{v}{\omega}\Gamma'_{10}\right)\left(e^{j\omega t_1} - 1\right)e^{j\Gamma'_{10}z} \qquad (94)$$

It is seen in Eq. (91) that this slot type kicker creats only a change in momentum in the verticle direction of the transverse plane. This result was derived based on the fact that TE_{10} waves were predominately excited in the kicker waveguide. It is obvious that if the beam guide dimensions were made in such a way that higher order modes such as TM_{11}, TM_{20} - - - - - etc. were excited, the interaction between the pickup and the kicker would be more than just affecting the transverse direction of current carriers, which are flowing in the center of beam chamber.

VIII. NUMERICAL RESULTS.

(A) Values for the pickup.

(1) Values for the beam chamber.

As seen in Eq. (9) that in order for waveguide modes to exist in the beam chamber, Γ'_{mn} must be real, i.e.

$$\Gamma'_{mn} = \sqrt{\beta_0^2 - \left(\frac{m\pi}{a}\right)^2 - \left(\frac{n\pi}{b}\right)^2} \qquad (9)$$

or

$$\beta_0^2 = \omega^2 \mu_r \epsilon_0 \geq \left(\frac{m\pi}{a}\right)^2 + \left(\frac{n\pi}{b}\right)^2 \qquad (95)$$

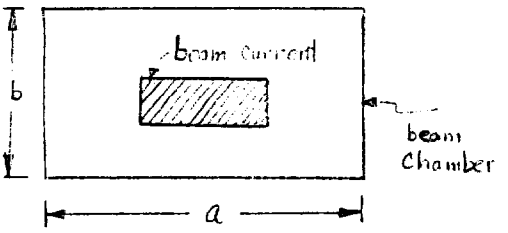

$a = 22.86\ cm = 9.''$

$b = 20.32\ cm = 8.''$

Fig. 9. Cross-Sectional dimensions of the beam chamber for the pick-up.

If the operating frequency is set at f = 1.0 MHz and dimension a and b are so chosen that only fundamental modes can propagate i.e. m = n = 1. It is found that one set of parameters for a and b to satisfy Eq. (95) is

$$\begin{cases} a = 22.86\ cm = 9.'' \\ b = 20.32\ cm = 8.'' \end{cases} \qquad (96)$$

(2) Values for the TEM Line.

The characteristic impendance and its inherent capacitance associated with a shield TEM line are well known [7]. In fact we could have calculated their values in Section V of this report by applying Gauss law. However, for experimental purposes, an approximated formula is sufficient. It is shown that the characterisic impedance of a TEM line (shown in Fig.10) is [8]

$$Z_0 = \frac{94.15}{\sqrt{\epsilon_r}\left[\frac{\ell}{c_2} + 1.63 - 1.18\,\frac{c_2}{b_2}\right]} \qquad (97)$$

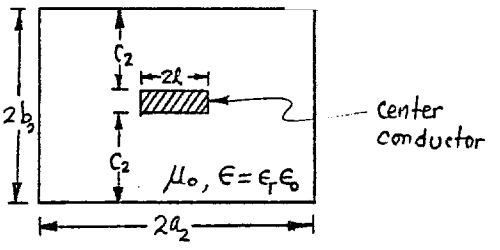

Fig.10.Dimensions of the TEM line

$2a_2 = 18.\ cm$

$2b_2 = 6.\ cm$

$c_2 = 2.75\ cm$

$2\ell = 2.74\ cm$

In order to match the speed of 200-MeV proton beam, it is easy to see that the dielectric constant $\epsilon_\gamma = 3.123$, and if $Z_0 = 50\Omega$. then

$$\begin{aligned} 2a_2 &= 18.\ cm \\ 2b_2 &= 6.\ cm \\ c_2 &= 2.75\,cm \\ 2\ell &= 2.74cm \\ \epsilon_\gamma &= 3.123 \end{aligned} \qquad (98)$$

(3) Numerical Results

It is seen throughout this analysis that, the Fourier current density, J_{mn}, of Eq. (16) plays an improtant role in all parts, thus it is of interest to consider its expressions for various cases. Since this current density expression enters mostly as J_{11} form, we shall repeat its expression for the case of square cross-sectional current here.

$$J_{11} = \frac{16 I_{z0}}{\pi^2 a_1 b_1} \sin\frac{\pi x_1}{a} \sin\frac{\pi a_1}{2a} \sin\frac{\pi y_1}{b} \sin\frac{\pi b_1}{2b}$$

$$+ \frac{16 I_{z0}}{\pi^2 a_1 b_1} \cos \nu\omega t \sin\frac{\pi x_1}{a} \sin\frac{\pi a_1}{2a} \cos\left(\frac{\pi y_1}{b}\right)\left(1 - \cos\frac{\pi b_1}{2b}\right)$$

$$= J_{11c} + J_{11p} \tag{99}$$

It is seen that this current consists of two parts, the one involved with e^{jnwt} and the other involved with $\cos \nu wt\ e^{jnwt}$. These two currents have different characteristics, in that J_{11c} is maximum when the center of this current density coincides with the center of the beam chamber, while J_{11p} is minimum in magnitude. These two currents are identificable because of their difference in frequence. Plots of these currents are shown in Figure 11 and 12. In Figure 11, a three-dimensional representation of J_{11c} is plotted. Parameters used for this figure are: Beam chamber dimensions a = 22.86 cm, b = 20.32 cm, and beam size a_1 = 4 cm, b_1 = 3 cm. In Figure 11, the magnitude of this beam current with cross-section area mentioned above is plotted against the location of the center of beam normalized to the sides of the beam chamber. It is seen that this current density is indeed maximum at the center of the chamber. Figure 12 is a similar plot with the same dimensions as shown in Figure 11 except that it is plotted for J_{11p}. Again, it is seen that the magnitude of this current density is zero at the center of the chamber and are maximum on the edges.

When m=n=1, the voltage in the center conductor of the TEM line is shown to be

$$V_0 = \frac{\frac{C_2}{2\ell} J_{11} \left(\frac{a}{b}\right)\sqrt{\frac{\mu_0}{\epsilon}} \left[\sin\frac{\pi}{a}(x_3 - a_3) - \sin\frac{\pi}{a}(x_3 + a_3)\right]}{(1+H)\left[\left(\frac{20\pi f}{3}\right)^2(\epsilon_r - 1) + \left(\frac{\pi}{a}\right)^2 + \left(\frac{\pi}{b}\right)^2\right]} \tag{100}$$

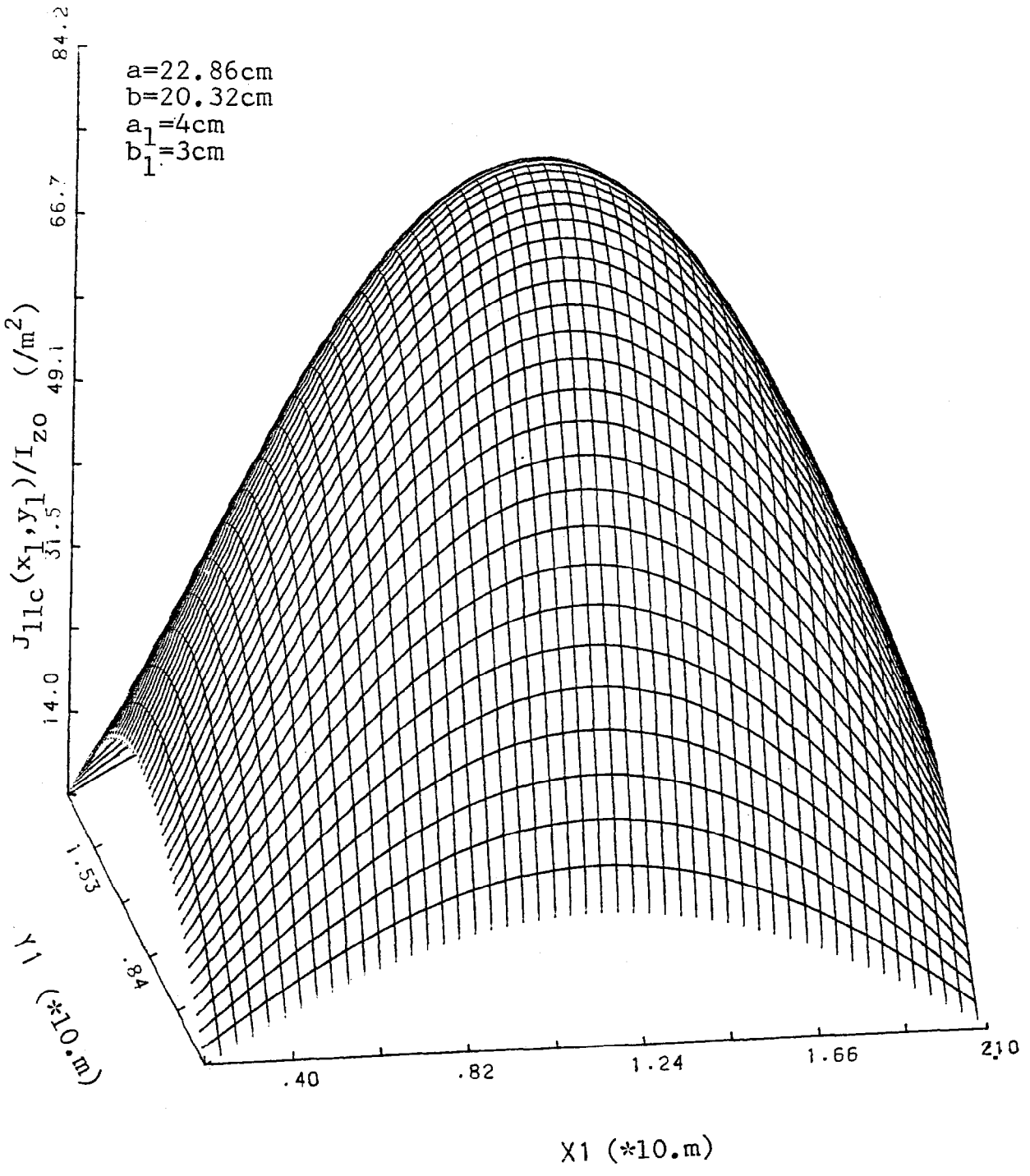

Fig. 11 Three dimensional representation of the common mode part of the Fourier current J_{11} as a function of x_1 and y_1, the location of the center of the rectangular beam current in the beam chamber. The maximum of the of the current is seen to be at the center of the chamber, i.e. $(x_1,y_1)=(a/2,b/2)$.

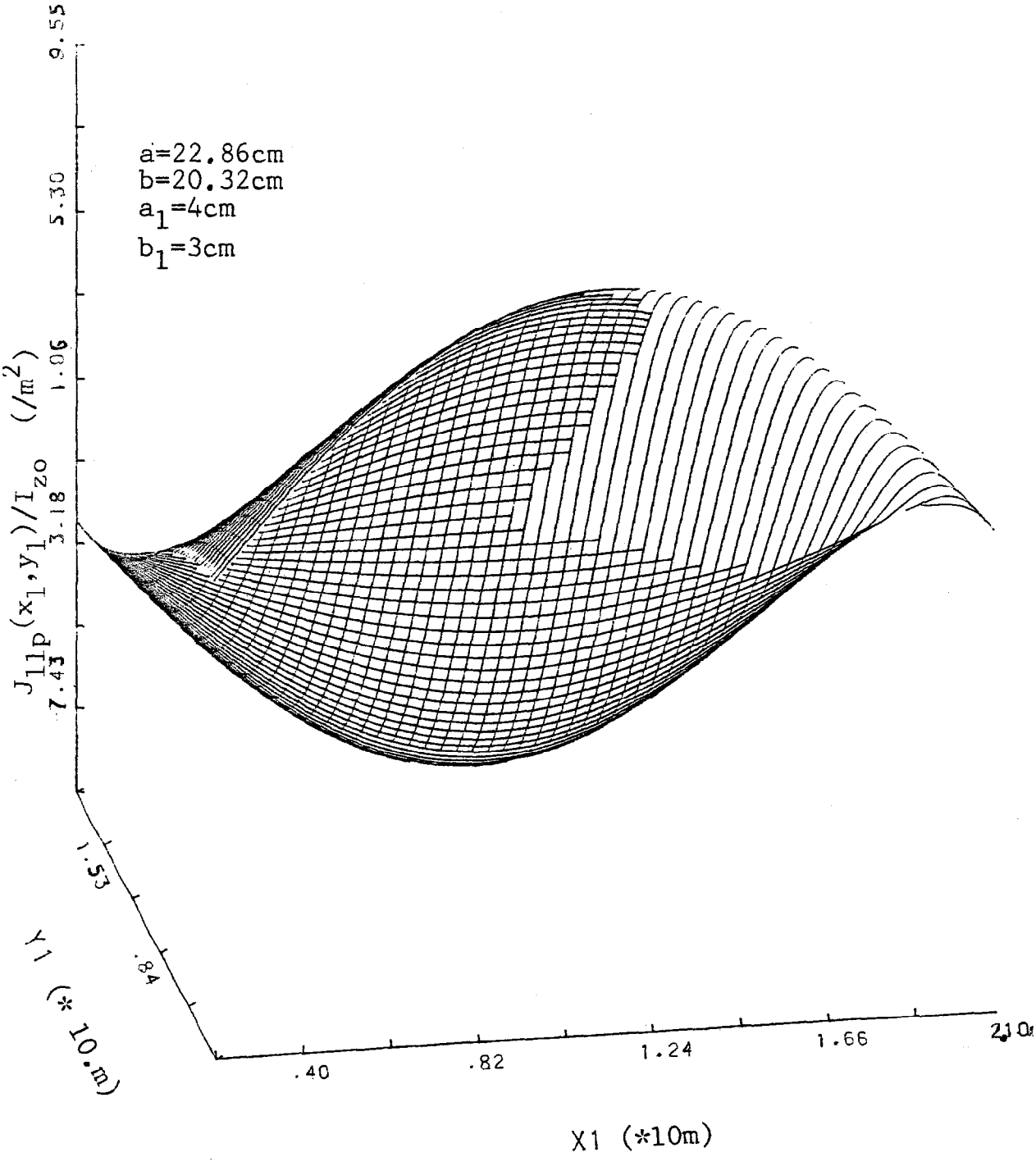

Fig. 12. Three dimensional representation of the push-pull part of the Fourier current J_{11} as a function of x_1 and y_1, the position of the center of the rectangular beam current in the beam chamber. Values of this current are seen to have opposite sign on the opposite edge in the Y direction and its value is zero when $(x_1,y_1)=(a/2,b/2)$

where f is in giga Hertz and

$$H = \sum_{m=1}^{\infty} \frac{c_2}{\ell} \frac{(-1)^m}{\pi} \left\{ \frac{2}{m} - \lim_{N\to\infty} \sum_{n=\text{odd}}^{2N-1} \frac{4\left[n^2 - \left(\frac{2b_2}{c_2}\right)^2\right]\left(\frac{b_2}{c_2}\right) m}{\left[n^2 - \left(\frac{2b_2}{c_2}\right)^2 m^2\right] N\left[n \coth\left(\frac{\pi \ell}{c_2}\right) \coth\left(\frac{n\pi}{2b_2}(a_2 - \ell) + \frac{2b_2}{c_2}\right)\right]} \right\}$$

$$- \frac{c_2}{2\ell} \lim_{N\to\infty} \sum_{n=\text{odd}}^{2N-1} \frac{\left[n^2 - \left(2b_2/c_2\right)^2\right]\left[2\cosh\frac{n\pi}{2b_2}(a_2 - \ell) - \cosh\frac{n\pi}{2b_2}(a_2 + x_3 - a_3) - \cosh\frac{n\pi}{2b_2}(a_2 - x_3 - a_3)\right]}{N\left(\frac{2b_2}{c_2}\right) \sin\left(\frac{n\pi c_2}{2b_2}\right)\left[n \coth\left(\frac{\pi \ell}{c_2}\right) + \frac{2b_2}{c_2} \tanh\frac{n\pi}{2b_2}(a_2 - \ell)\right]} \qquad (101$$

A plot of $|V_o/I_{zo}|$ versus x_3 is shown in Figure 13. In this figure, parameters used are: a = 22.32 cm, a_2 = 9. cm, b_2 = 3 cm, c_2 = 2.75 cm and ℓ = 1.371 cm, b=20.32cm a_3 = 8.5 cm and x_3 varies from zero (center of the slot and the beam chamber in x- direction) to $(a_2 - a_3)$ = 0.5 cm and its value is normalized to a. It is seen that $|V_o/I_{zo}|$ increases as the center of the slot is moved away from the center of TEM line or the beam chamber in the x- direction. The effect of this increment is believed to be due to a increase in the forward power flow in the TEM line. Further computer simulation shows that $|V_o/I_{zo}|$ changes as x_3 approaches the value of ℓ. These flutuations in $|V_o/I_{zo}|$ are believed to be caused by a change in power flow in the TEM line and the power coupling between the beam guide and the TEM line.

Variation of $|V_o/I_{zo}|$ as a function of a_3, the length of the slot is shown in Figure 14. In this figure, parameters in Figure 13 were used, except that at this time, we used x_3 = 0, and a_3 is varied from 2 cm, to 8.5 cm, and normalized to a. It is seen that $|V_o/I_{zo}|$ increases as a_3 increases. This effect is easy to visualize. For as a_3 increases, more power is coupled through the hole from the beam chamber to the TEM line.

It is instructive to consider the field configurations in the TEM line for a coupled power from the beam chamber. This is shown in Figures 15 and 16. In these figures, electric field intensity E_x and E_y in the TEM line were plotted. Expressions in Eq. (51) were plotted in a 3-dimensional representation fashion, in that field intensity normalized to V_o were plotted as a function of position x and y in one-quarter of TEM line. One-quarter of the cross-section is plotted because the fields are symmetric in the other three quarters. Parameters in these figures are the same as we used in the previous figures. It is seen that these field intensities

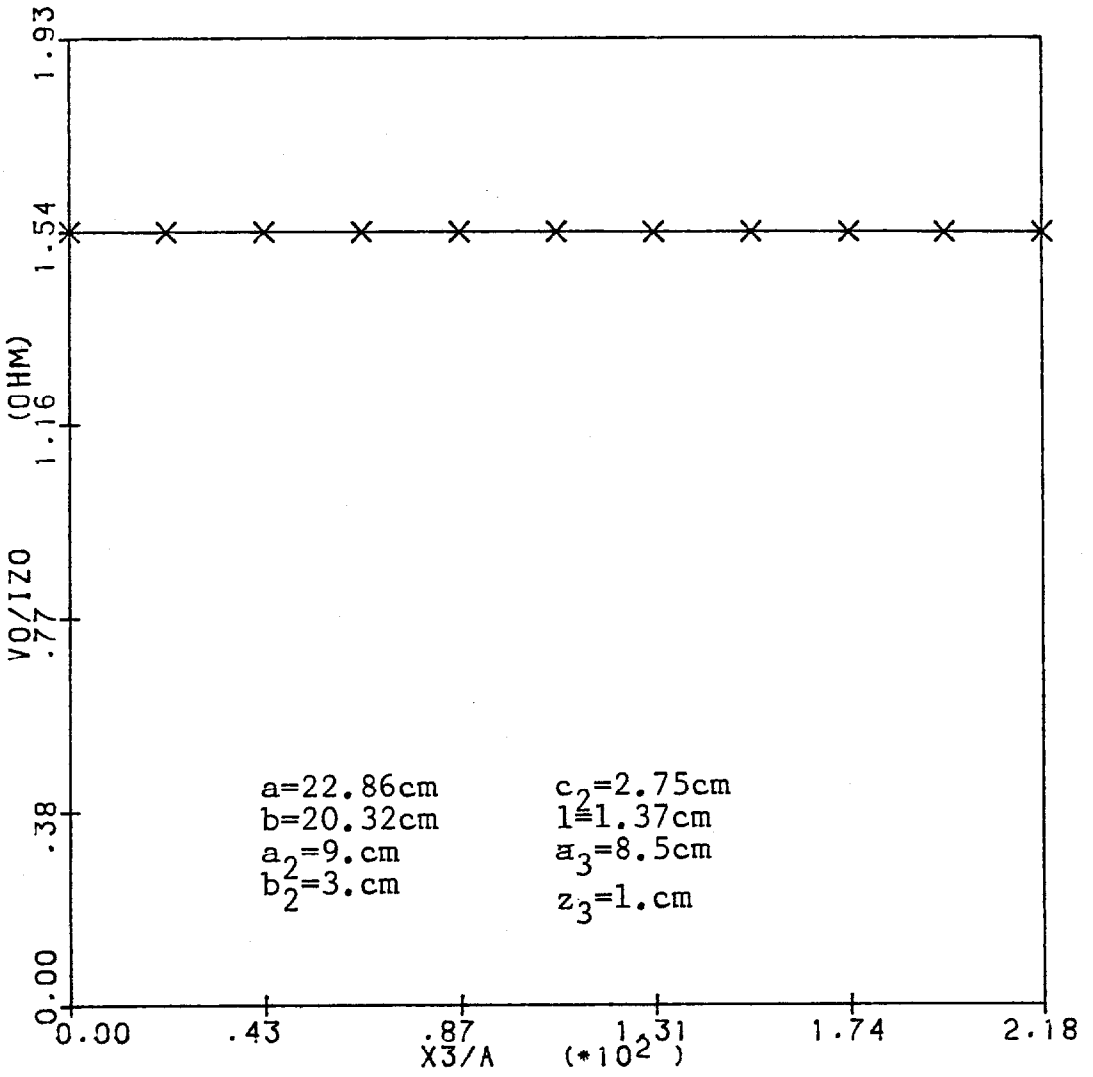

Fig. 13. Voltage induced on the center conductor of TEM line, V_o, normalized to the magnitude of the beam current, I_{zo}, as a function of the center position of the slot relative to the broad side wall of the beam chamber.

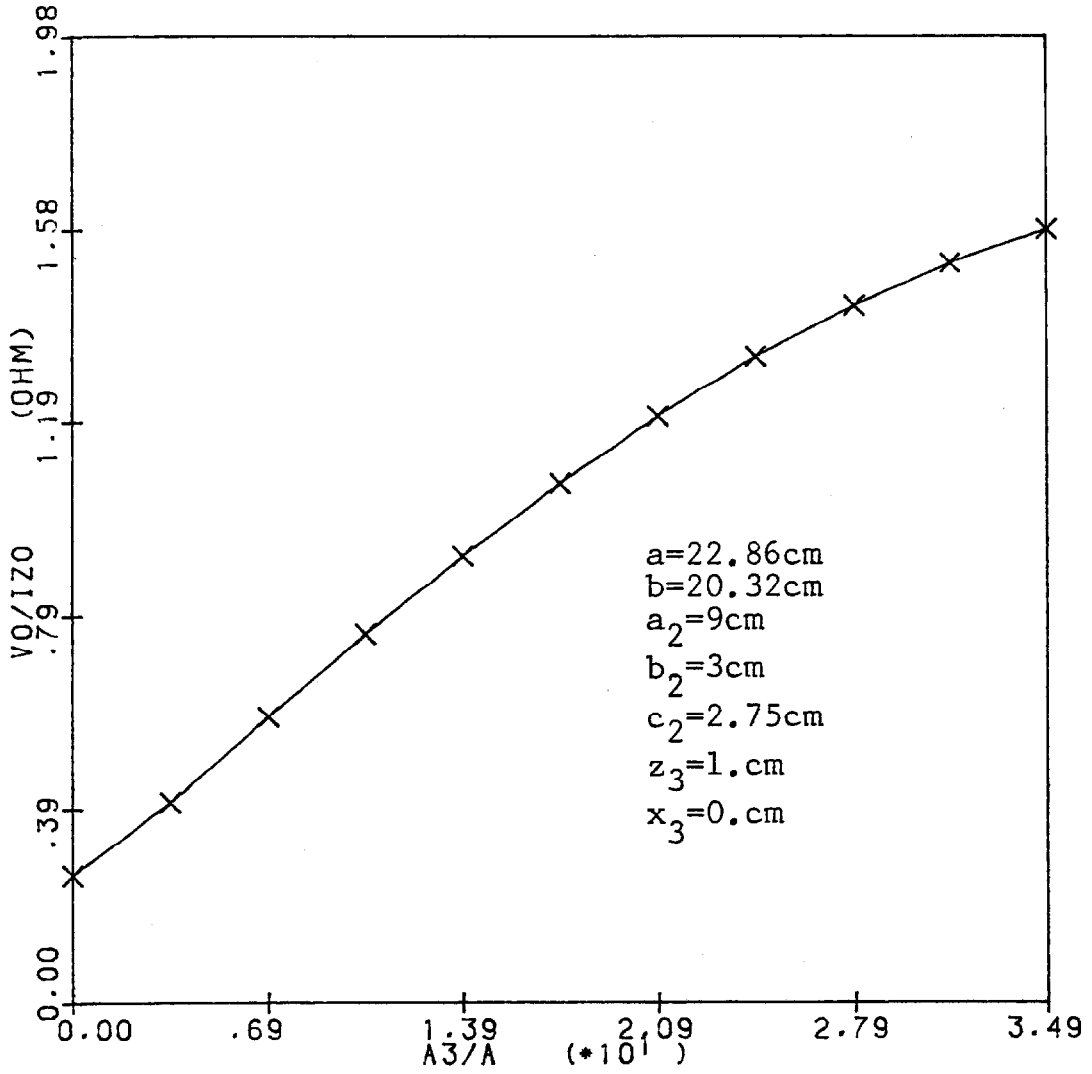

Fig. 14. Voltage, V_o, induced on the center conductor of the TEM line, normalized to the magnitude of the beam current, I_{zo}, as a function of the size of the slot, a_3, normalized to a.

peak at various locations throughout the cross-sectional area of the TEM line. These scattered multiple peak values are believed to be caused by multi-mode fields in the TEM line. However, no matter how these fields behave in the cross-section, their electric field intensities are zero on the conducting boundaries, as they are required. Plots for the magnetic fields are unnecessary, because they differ from the electric fields by a constant -- indicated in Eq. (52).

Last, but not least, the equivalent transfer resistance (Eq. 74) R_T is plotted as a function of x_3 and a_3. These are shown in Figures 17, 18 and 19. In Figure 17, transfer resistance due to one slot was plotted as a function of x_3. Parameters used in this figure are the same as that used in Figure 13. It is seen in Figure 17 that this resistance is fairly constant as x_3 varies. This is so because x_3 varied in a relatively small range. In Figure 18, similar plot is shown. In this case, a_2 is enlarged to 20. cm while the characteristic impedance of the TEM line still maintained at 50 Ohms. Thus, in this case, values of x_3 varied in a larger range (from zero to 1.233 cm). It is seen that in this case R_T changes rather rapidly as x_3 approaches the value of ℓ (= 1.37 cm) and peaks at some points. Thus, this allows us to pick an optimum value of x_3 such that maximum power transfer is obtained. Figure 19 is a similar plot except that this transfer resistance is plotted against the size of the slot in the transverse direction (a_3). It is clear from Eq. (73) that this value increases at a rate that corresponds to the 6th power of a_3. This effect is obvious for the larger the slot, the higher the power will transfer so long as the small power coupling assumption is not violated. It is interesting to note that maximum power coupling corresponds to a slot opening located on a spot where maximum field exists in the beam chamber.

(B) Values for the Kicker

Since we are interested in the lowest possible waveguide mode in the kicker, we could make the beam chamber as small as possible. In the previous analysis (Section VIII), we assumed TE_{10} mode prevailed in the beam guide. Thus, for an operating frequency of 1 GH_z, dimension for the beam guide can be made as follows: (See Figure 20)

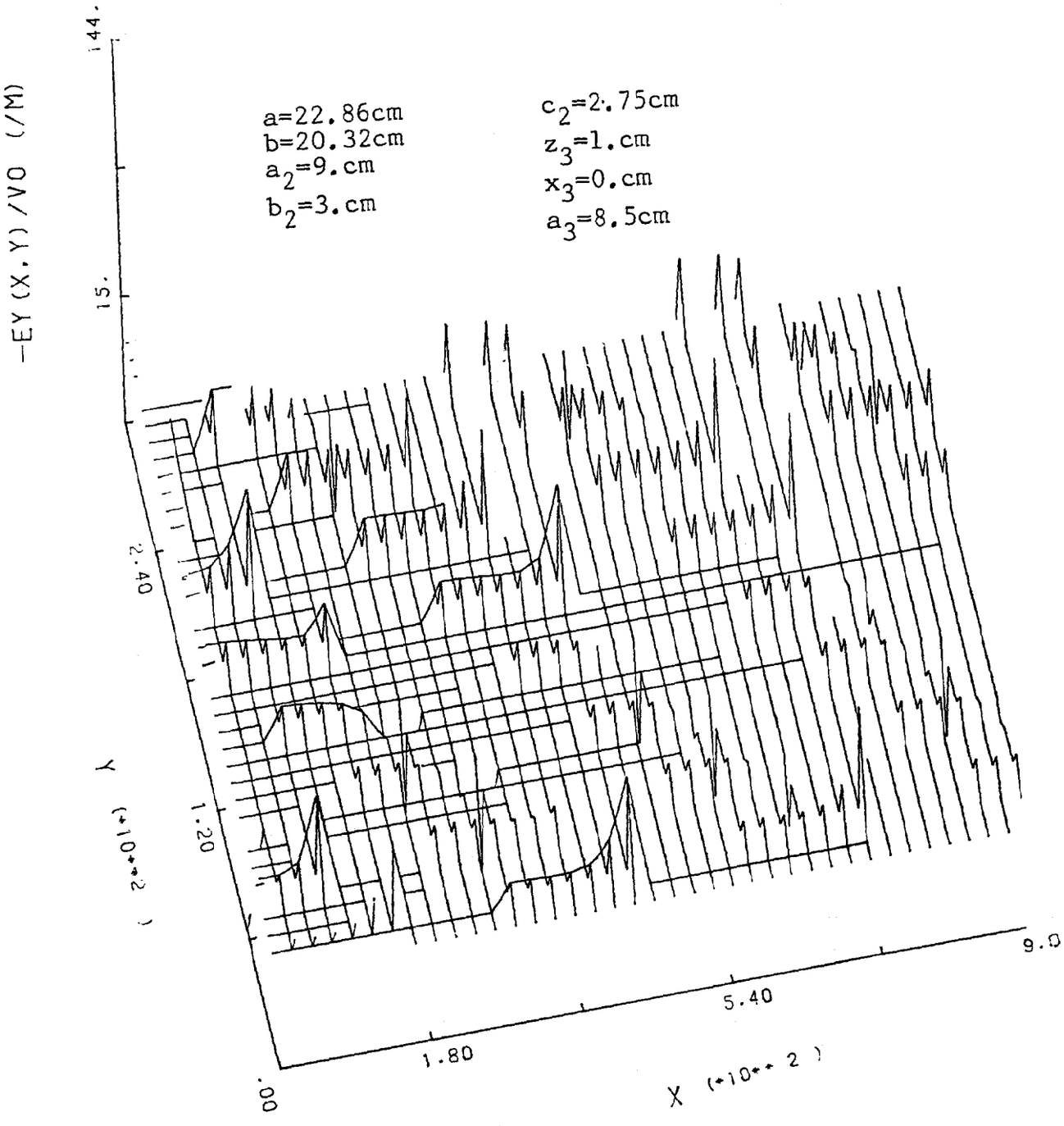

Fig. 16. A three dimensional representation of the electric field intensity $E_y(x,y)$ in the TEM line as a function of x and y.

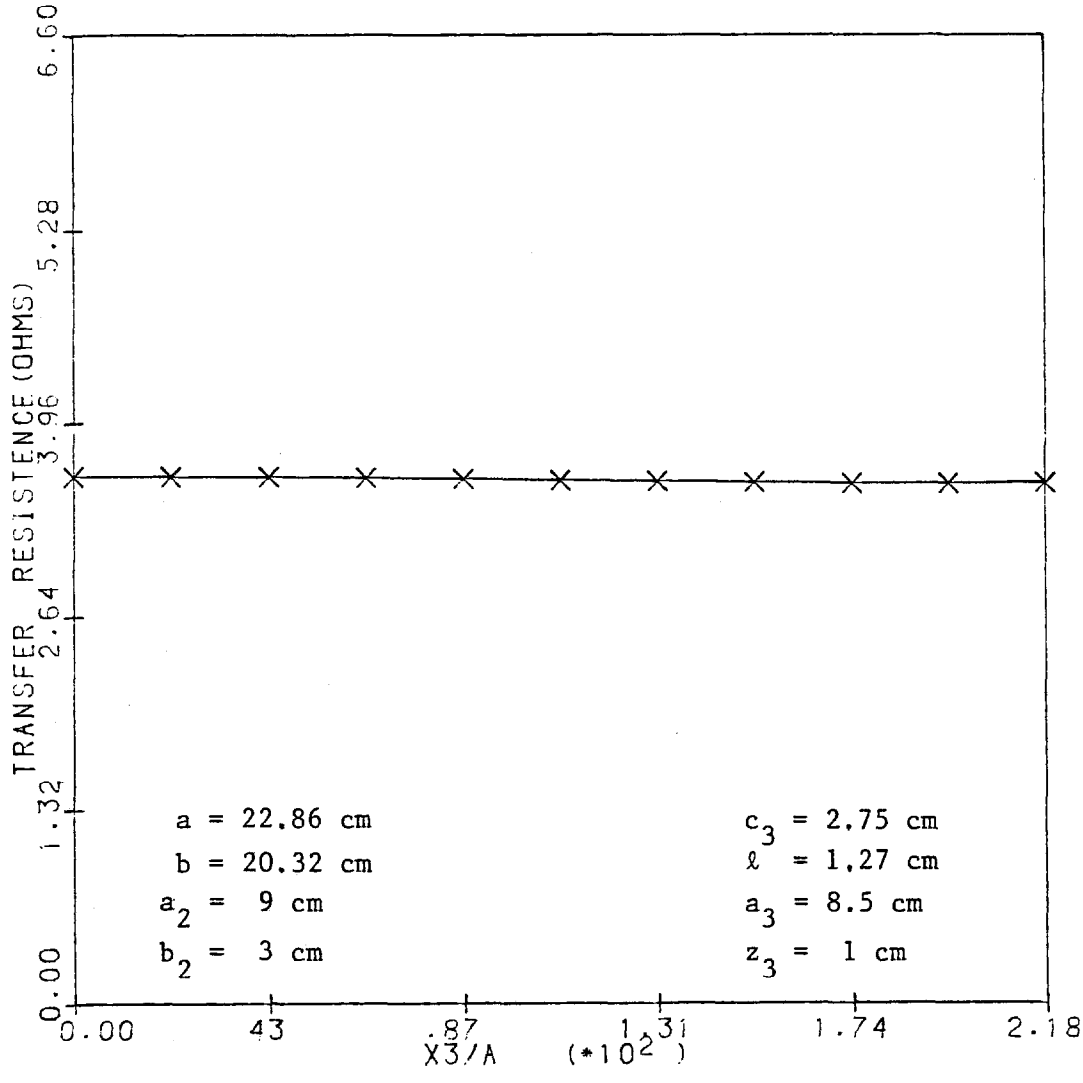

Fig. 17. Equivalent transfer resistance R_T as a function of the slot center x_3 away from the center line of the beam chamber.

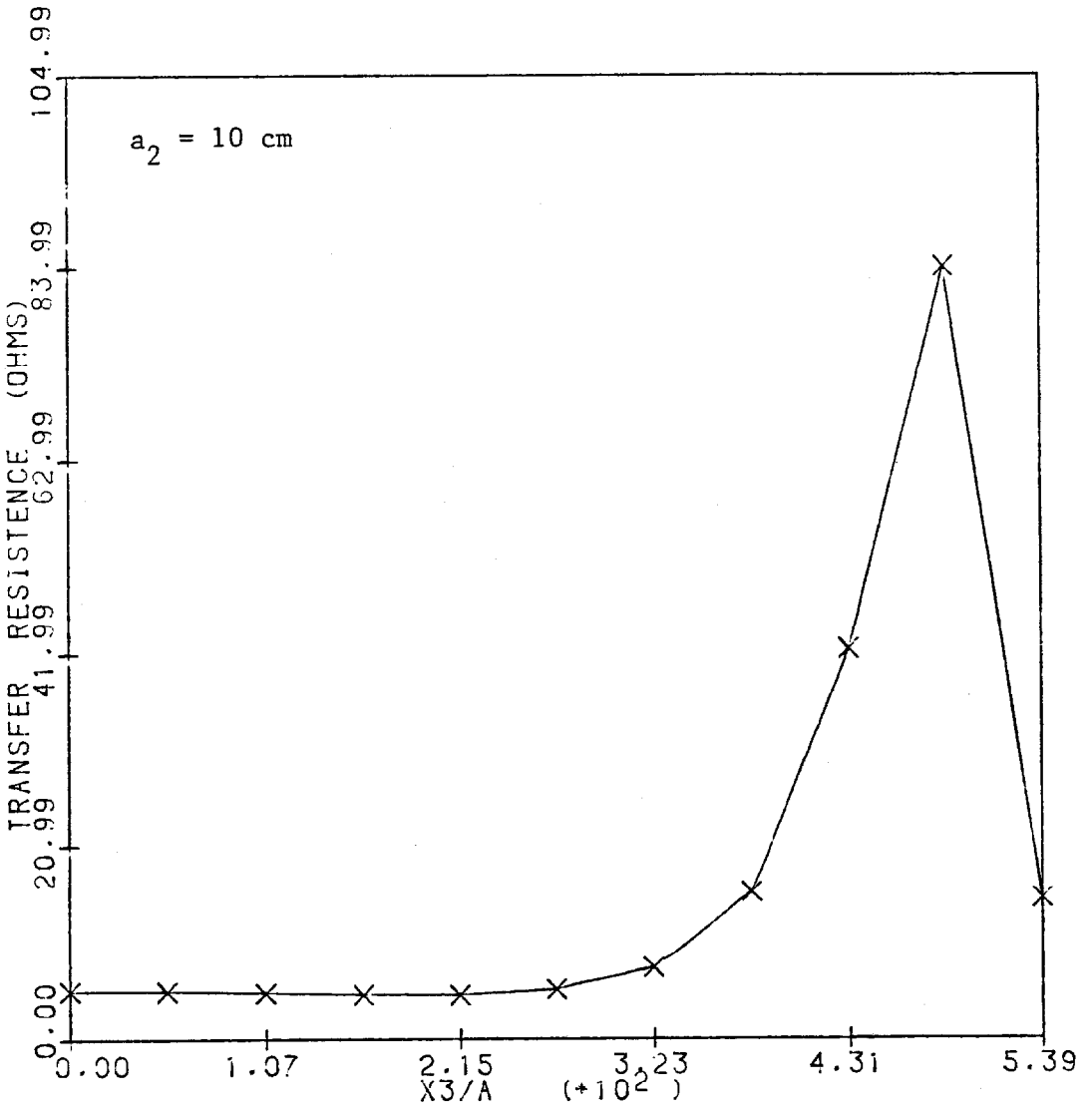

Fig. 18. Equivalent transfer resistance R_T as a function of the slot center x_3 away from the center line of the beam chamber. Parameters used in this figure is the same as that used in Fig. 17 except that a_2 is increased to 10 cm so that the value of x_3 can vary in a larger range.

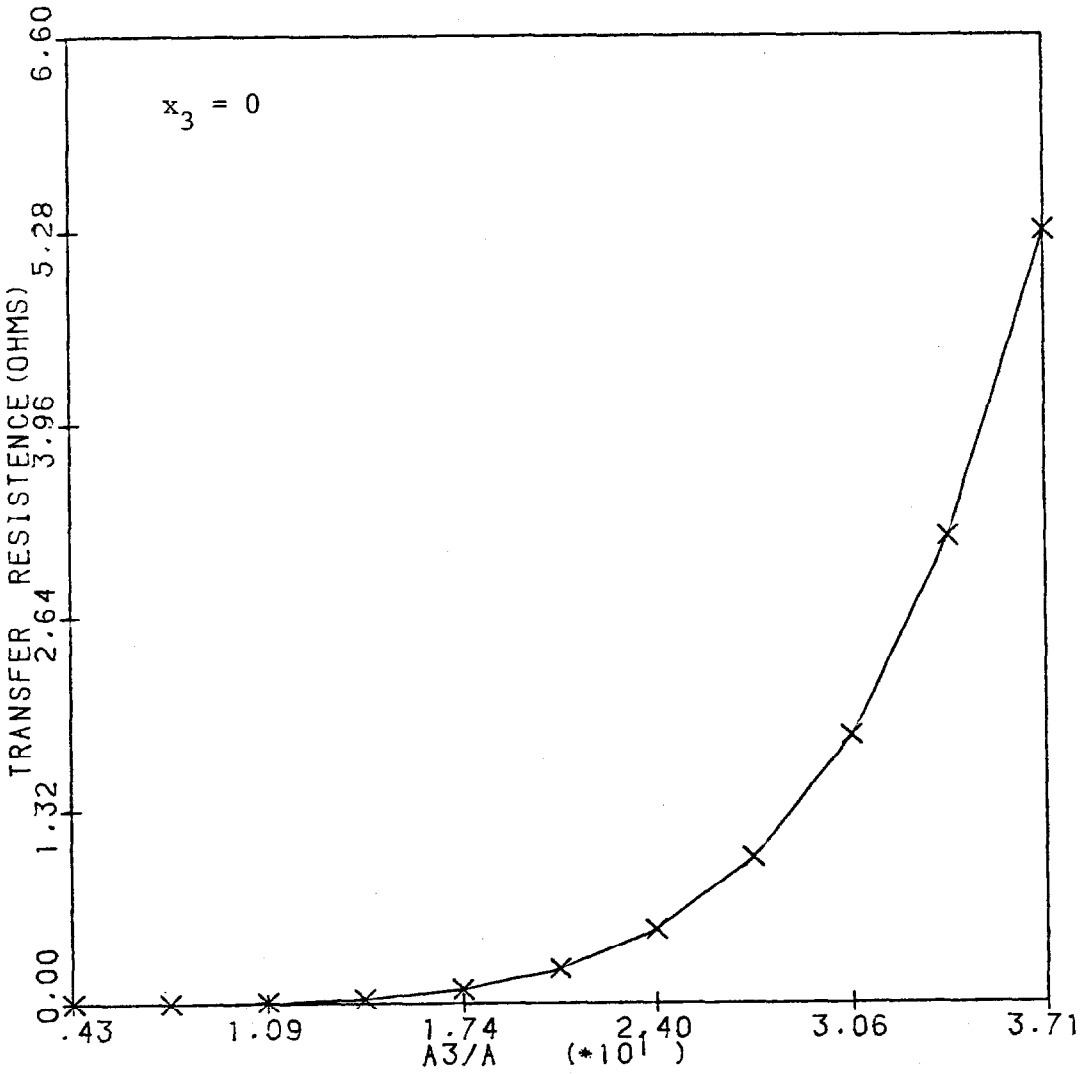

Fig. 19. Equivalent transfer resistance R_T as a function of the size of slot size. Parameters used in this figure is the same as that used in figure 17 except that here $x_3 = 0$, and a_3 varies in an interval from 1. to 8.5 cm.

$$a = 15.5 \text{ cm}$$
$$b = 10 \text{ cm} \qquad (102)$$

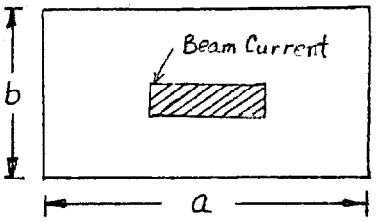

$a = 15.5\,cm$, $b = 10.\,cm$

Fig. 20. Beam chamber Dimensions for the Kicker.

As for the TEM line associated with the kicker, in view of Eq. (97), one can make it with the following dimensions while a characteristic impedance of 50 Ω is still maintained: (Figure 21)

$$a_2 = 10 \text{ cm}$$
$$b_2 = 4 \text{ cm}$$
$$\ell = 1.96 \text{ cm}$$

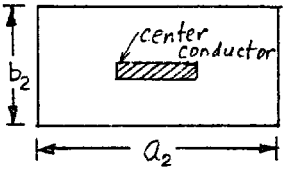

Fig. 21. TEM line dimensions for the Kicker.

Numerical results for the kicker can be inferred from previous sections.

X. Summary and Discussion.

Theory and numerical dimensions for a design of a slot type pick-up and kicker for stochastic cooling experiment have been presented in this report. Waveguide field in the beam chamber and TEM waves in the TEM-coupled line were derived in detail. It is shown that when dimensions are properly designed, TM_{11} is excited in the beam chamber. Longitudinal component, as well as other transverse components, of the electric field were shown to be present in the beam chamber. It was also shown that this longitudinal component was still non-zero even when the velocity of the beam particles approached the velocity of light. For this corresponds to a case in which the beam possesses an infinitely large energy and a slight modification of the beam velocity will contribute enough energy (or power) to coupling. Because of this longitudinal component of the electric field, signals will be induced on any conductor, which is oriented in the longitudinal direction with respect to the beam-flow direction. This analysis can be generalized to all types of waveguide type pick-ups and kickers. It is interesting to observe, at this juncture, that the longitudinal and vertical pick-up and kicker, built by the Berkeley people[1] were built on the same principle — a Traveling Wave Tube type (or a helix) conductor within a circular beam chamber. Thus, cylindrical waves in the waveguide were induced on the conductor of the helix. On the other hand, this structure will encounter mechanical difficulties when the beam velocity approaches the velocity of light, in that case, a helix becomes a straight line.

Fields in the TEM line were derived in detail in this report. Exact field configurations for these fields were also found. Power coupling factor between the beam

chamber and the TEM line were derived in detail. It was shown in Figure 13 that a voltage coupling of value ranging from 1 to 10 was obtained. Single slot coupling as well as multi-slot coupling was also derived. It was shown that a power coupling (or an equivalent transfer resistance) coefficients for the single slot coupling can obtain a modest value of 5 ohms, and as high as 100 ohms. This power coupling is shown to be linear in the system, hence, if 30 slots are used in each electrode, a 150-ohm transfer resistance is obtained for the system. If the slots are separated by 3 cm apart, the total active coupling region corresponds to about 1 meter. This, thus, corresponds to a 150-ohm/meter pick-up or kicker system, a considerable promising result.

Values for the kicker were also derived in this report. It was shown that vertical momentum of the beam carrier was affected if the beam chamber was so designed that only TE_{10} mode was allowed to be excited.

Numerical values as well as configurations, dimensions, of each component of the system were given in details in the report.

The bandwidth associated with this slot type pickup or kicker depends on the conducting losses associated with the waveguide and the TEM line walls [12], the size of the slots, and the electrical connectors to the system. For copper walls and dimensions of the system we were using, tens or hundreds of megahertz bandwidth is not unusual.

One other problem we have not addressed is reflections of the waveguide fields at the ends of the beam chamber. This problem can be overcome by extending the beam chamber for a certain length beyond the active region and by coating these extended surfaces by lossy materials to dissipate the current. It was shown by Faltin [3] that 20 dB/m lossy coating is sufficient to suppress the unwanted reflected wave. As far as higher order waveguide mode damping is concerned, filter type damping material is needed.

APPENDIX A

As shown in Eq. (33), we want to evaluate the integral

$$I = \int_{x_1 - \frac{a_1}{2}}^{x_1 + \frac{a_1}{2}} \sin\left(\frac{m\pi x}{a}\right) \cos\left[\frac{n\pi}{b}\left(y_1 + \frac{b_1}{a_1}\sqrt{a_1^2 - (x - x_1)^2}\right)\right] dx$$

$$= \int_{x_1 - \frac{a_1}{2}}^{x_1 + \frac{a_1}{2}} \frac{1}{2}\left[\sin\left(\frac{n\pi y_1}{b} + \frac{n\pi b_1}{b a_1}\sqrt{a_1^2 - (x - x_1)^2} + \frac{m\pi x}{a}\right)\right. \tag{A1}$$

$$\left. - \sin\left(\frac{n\pi y_1}{b} + \frac{n\pi b_1}{b a_1}\sqrt{a_1^2 - (x - x_1)^2} - \frac{m\pi x}{a}\right)\right] dx$$

with $u = x - x_1$ then $du = dx$, $x = u = x_1$ and

$$I = \int_{-\frac{a_1}{2}}^{\frac{a_1}{2}} \frac{1}{2}\left\{\sin\left[\frac{n\pi b_1}{b a_1}\sqrt{a_1^2 - u^2} + \frac{m\pi u}{a} + \frac{n\pi y_1}{b} + \frac{m\pi x_1}{a}\right]\right.$$

$$\left. - \sin\left[\sin\left[\frac{n\pi b_1}{b a_1}\sqrt{a_1^2 - u^2} - \frac{m\pi u}{a} + \left(\frac{n\pi y_1}{b} - \frac{m\pi x_1}{a}\right)\right]\right]\right\} du$$

$$= \int_{-\frac{a_1}{2}}^{\frac{a_1}{2}} \frac{1}{2}\sin\left[\left(e\sqrt{a_1^2 - u^2} + fu\right) + g\right] du$$

$$- \frac{1}{2}\int_{-\frac{a_1}{2}}^{\frac{a_1}{2}} \sin\left[\left(e\sqrt{a_1^2 - u^2} - fu\right) + h\right] du \tag{A2}$$

where

$$\begin{cases} e = \dfrac{n\pi b_1}{a_1 b}, \quad f = \dfrac{m\pi}{a}, \quad g = \dfrac{n\pi y_1}{b} + \dfrac{m\pi x_1}{a} \\ \\ h = \dfrac{n\pi y_1}{b} - \dfrac{m\pi x_1}{a} \end{cases} \tag{A3}$$

Thus

$$I = \frac{1}{2}\int_{-\frac{a_1}{2}}^{\frac{a_1}{2}} \left\{ \sin\left[e\sqrt{a_1^2-u^2} + fu\right] \cos g + \cos\left[e\sqrt{a_1^2-u^2} + fu\right] \sin g \right\} du$$

$$-\frac{1}{2}\int_{-a_1/2}^{a_1/2} \left\{ \sin\left[e\sqrt{a_1^2-u^2} - fu\right] \cos h + \cos\left[e\sqrt{a_1^2-u^2} - fu\right] \sin h \right\} du \qquad \text{(A4)}$$

If we let $u = a_1 \cdot \sin\theta$, then $du = a_1 \cos\theta \, d\theta$ and

$$I_1 = \int_{-a_1/2}^{a_1/2} \cos\left[e\sqrt{a_1^2-u^2} + fu\right] du$$

$$= \int_{-\frac{\pi}{2}}^{\frac{\pi}{2}} \cos\left[e\, a_1 \cos\theta + a_1 f \sin\theta\right] a_1 \cos\theta \, d\theta$$

$$= \int_{-\frac{\pi}{2}}^{\frac{\pi}{2}} \cos\left[a_1\sqrt{e^2+f^2}\left(\frac{e}{\sqrt{e^2+f^2}}\cos\theta + \frac{f}{\sqrt{e^2+f^2}}\sin\theta\right)\right] a_1 \cos\theta \, d\theta$$

$$= \int_{-\frac{\pi}{2}}^{\frac{\pi}{2}} \cos\left[z\cos(\theta-\phi)\right] a_1 \cos\theta \, d\theta \qquad \text{(A5)}$$

where

$$z = a_1\sqrt{e^2+f^2} = a_1 \pi \sqrt{\frac{n^2 b_1^2}{a_1^2 b^2} + \frac{m^2}{a^2}} \quad , \quad \tan^{-1}(\phi) = \frac{f}{e} \qquad \text{(A6)}$$

now, let $\psi = \theta - \phi$, then $\theta = \psi + \phi$ and $d\theta = d\psi$ and

$$I_1 = \int_{-\frac{\pi}{2}-\phi}^{\frac{\pi}{2}-\phi} \cos\left[z\cos\psi\right] a_1 \cos\left[\psi+\phi\right] d\psi$$

$$= \int_{-\frac{\pi}{2}-\phi}^{\frac{\pi}{2}-\phi} \cos\left[z\cos\psi\right] a_1 \left[\cos\psi\cos\phi - \sin\psi\sin\phi\right] d\psi$$

$$= a_1 \cos\phi \int_{-\frac{\pi}{2}-\phi}^{\frac{\pi}{2}-\phi} \cos[z\cos\psi]\cos\psi \, d\psi$$

$$- a_1 \sin\phi \int_{-\frac{\pi}{2}-\phi}^{\frac{\pi}{2}-\phi} \cos[z\cos\psi]\sin\psi \, d\psi$$

$$= \frac{a_1 \sin\phi}{z} \sin[z\cos\psi]\Big|_{\psi=-\frac{\pi}{2}-\phi}^{\psi=\frac{\pi}{2}-\phi} + a_1\cos\phi \int_{-\frac{\pi}{2}-\phi}^{\frac{\pi}{2}-\phi} \cos[z\cos\psi]\cos\psi \, d\psi$$

$$= \frac{2a_1 \sin\phi}{z} \sin[z\sin\phi] + a_1 \cos\phi \int_{-\frac{\pi}{2}-\phi}^{\frac{\pi}{2}-\phi} \cos[z\cos\psi]\cos\psi \, d\psi$$

$$= \frac{2a_1 \sin\phi}{z} \sin[z\sin\phi] + 2a_1 \cos^2\phi \, J_0(z) \qquad \text{(A7)}$$

where $J_0(Z)$ is the Bessel function of the first kind and zero order. The second term is derived in Appendix B.

Similarly, with θ substituted by $-\theta$, we have

$$I_2 = \int_{-\frac{a_1}{2}}^{\frac{a_1}{2}} \cos\left[e\sqrt{a_1^2-u^2} - fu\right] du$$

$$= \frac{2a_1 \sin\phi}{z} \sin[z\sin\phi] + 2a_1\cos^2\phi \, J_0(z) \qquad \text{(A8)}$$

Similarly, it can be shown that

$$I_3 = \int_{-\frac{a_1}{2}}^{\frac{a_1}{2}} \sin\left[e\sqrt{a_1^2-u^2} + fu\right] du$$

$$= \int_{-\frac{\pi}{2}-\phi}^{\frac{\pi}{2}-\phi} a_1 \cos\phi \sin[z\cos\psi]\cos\psi \, d\psi$$

$$- a_1 \sin\phi \int_{-\frac{\pi}{2}-\phi}^{\frac{\pi}{2}-\phi} \sin[z\cos\psi]\sin\psi \, d\psi \qquad \text{(A9)}$$

$$= \int_{-\frac{\pi}{2}-\phi}^{\frac{\pi}{2}-\phi} a_1 \cos\phi \sin[z\cos\psi]\cos\psi \, d\psi$$

$$= 0 \qquad \text{(A9)}$$

Result for Eq. (A9) is derived in Appendix B in details.

and

$$I_4 = \int_{-\frac{a_1}{2}}^{\frac{a_1}{2}} \sin[e\sqrt{a_1^2-u^2} - fu]\, du = 0$$

Thus, Eq. (A-4) becomes

$$I = (\sin g - \sin h)\left\{\frac{a_1 \sin\phi}{z}\sin[z\sin\phi] + a_1\cos^2\phi\, J_0(z)\right\} \qquad \text{(A10)}$$

$$+ \frac{a_1}{2}\cos\phi\, J_1(z)[\cos y - \cos h]$$

with g, h, z and Θ are defined in (A-3) and (A-5)

The integration

$$I_5 = \int_{x_1-\frac{a_1}{2}}^{x_1+\frac{a_1}{2}} \sin\left(\frac{m\pi x}{a}\right)\cos\left[\frac{n\pi}{b}\left(y_1 - \frac{b_1}{a_1}\sqrt{a_1^2-(x-x_1)^2}\right)\right] dx \qquad \text{(A11)}$$

is the same as given in Eq.(A1) except that now e is negative, or ϕ is replaced by $(\pi-\phi)$, i.e.

$$\phi' = \pi - \phi$$

Thus,

$$I_5 = (\sin g - \sin h)\left\{\frac{a_1\sin\phi}{z}\sin(z\sin\phi) + a_1\cos^2\phi\, J_0(z)\right\}$$

$$- \frac{a_1}{2}\cos\phi\, J_1(z)[\cos g - \cos h] \qquad \text{(A12)}$$

APPENDIX B

In this appendix, we would like to evaluate the integration:

$$I = \int_{-\frac{\pi}{2}-\phi}^{\frac{\pi}{2}-\phi} \cos(z\cos\psi)\cos\psi\, d\psi \tag{B1}$$

Before we do that, let us review the following formulas*

$$\int_{-\frac{\pi}{2}-\phi}^{\frac{\pi}{2}-\phi} \cos m\theta \cos n\theta\, d\theta = \int_0^{\pi} \cos m\theta \cos n\theta\, d\theta$$

$$= \begin{cases} 0 & \text{if } m \neq n \\ \frac{\pi}{2} & \text{if } m = n \end{cases} \tag{B2}$$

and it can be shown †

$$\cos(z\cos\psi) = J_0(z) + 2\sum_{k=1}^{\infty}(-1)^k J_{2k}(z)\cos(2k\psi) \tag{B3}$$

where J_k are Bessel functions of the first kind, order k.

Thus,
$$I_1 = \int_{-\frac{\pi}{2}-\phi}^{\frac{\pi}{2}-\phi} J_0(z)\cos\psi\, d\psi$$

$$= 2\, J_0(z)\cos\phi \tag{B4}$$

Similarly, it can be shown that

$$\sin(z\cos\theta) = 2\sum_{k=0}^{\infty}(-1)^k J_{2k+1}(z)\cos[(2k+1)\theta] \tag{B5}$$

Thus
$$\int_{-\frac{\pi}{2}-\phi}^{\frac{\pi}{2}-\phi} \sin[z\cos\psi]\cos\psi\, d\psi = J_1(z) \tag{B6}$$

---

* For example, see "Tables of Integrals and Other Mathematical Data" by H.B. Dwight, MacMillan, Inc. (1961).

† M. Abramowitz and I.A. Stegun, "Handbook of Mathematical Functions". Dover Pub. Inc. p. 361, (1965).

REFERENCES

[1] G. Lambertson, J. Bisognano, W. Flood, L. J. Laslett, C. Leemann, B. Leskovar, C. C. Lo, R. Main, L. Smith, and J. Staples, " Stochastic Cooling of 200-MeV Protons, "$\bar{p}$ Note 81, Lawrence Berkeley Lab., Berkeley, CA 94720.

[2] P. Bramham, G. Carron, K. Hubner, W. Schnell and L. Thorndahl, "Stochastic Cooling of a Stored Proton Beam," Nuclear Instr. and Meth. 125, 201-202 (1975).

[3] L. Faltin, "Slot Type Pick-up and Kicker for Stochastic Beam Cooling," Nuclear Inst. and Meth., 148, 449-455 (1978).

[4] S. A. Schelkumoff, Electromagnetic Waves, 10th Printing, (D. Van Nostrand Co., New York, 1960) Chap. 10.

[5] L. Faltin, "RF Fields Due to Schottky Noise in a Coasting Particle Beam," Nuclear Inst. and Meth., 145, 261-266 (1977).

[6] J. R. Pierce, Traveling-Wave Tubes, (D. Van Nostrand Co, New York, 1950).

[7] N. A. Begovich, "Capacity and Charateristic Impedance of Strip Transmission Lines with Rectangular Inner Conductors," IRE Trans. on MTT-3, 127-133 (1955).

[8] R. N. Ghose, Microwave Circuit Theory and Analysis, (McGraw-Hill Book Co, 1963), pp. 113-116.

[9] R. E. Collin, Field Theory of Guided Waves, (McGraw-Hill, New York, 1960).

[10] L. J. Laslett, V. K. Neil and A. M. Sessler, "Transverse Resistive Instabilities of Intense Coasting Beams in Particle Accelerators," Rev. of Sci. Inst. 36, 436-448, (1965).

[11] E. Keil and Zotter, "Longitudinal Stability of a Coasting Beam in a Corrugated Resistive Vacuum Chamber," Particle Acc., 3, 11-20, (1972).

[12] R. E. Collin, Foundations for Microwave Engineering, (McGraw-Hill, New York 1966).

[13] S. B. Cohn, "Determination of Aperture Parameters by Electrolytic-Tank Measurements," Proc. IRE, 1416-1421, (1951).

[14] C. Montgomery, R. Dicke and E. Purcell, Principles of Microwave Circuits, 8th Ed. (McGraw-Hill Book Co., New York, 1948), p. 178.

[15] L. D. Landau and E. M. Lifshitz, The Classical Theory of Fields, Rev. 2nd ed. (Addison-Wesley Co., Massachusetts, 1965), Chap. 3.